

Hailu, Sofonias Amdemariam

**Dynamic Inter-operator Spectrum
Sharing Between Co-located Radio
Access Networks Using Cooperation
Transmission**

School of Electrical Engineering

Thesis submitted for examination for the degree of Master of
Science in Technology.

Espoo, Jan 20, 2014

Thesis supervisor:

Prof. Olav Tirkkonen

Thesis instructor:

Dr. Alexis Dowhuszko

Author: Hailu, Sofonias Amdemariam		
Title: Dynamic Inter-operator Spectrum Sharing Between Co-located Radio Access Networks Using Cooperation Transmission		
Date: Jan 20, 2014	Language: English	Number of pages:9+56
School of Electrical Engineering Department of Communications and Networking Technologies Professorship: Radio Communications		Code: S-72
Supervisor: Prof. Olav Tirkkonen		
Instructor: Dr. Alexis Dowhuszko		
<p>Increasing the operational bandwidth is crucial to improve the capacity of future mobile networks and cope with the ever increasing demand of mobile data. One viable option to increase the operational bandwidth is through inter-operator spectrum sharing. The main idea behind this concept is that operators share part of their spectrum in orthogonal or non-orthogonal ways. In orthogonal spectrum sharing, only a single operator is allowed to access a given frequency resource at a time, whereas in non-orthogonal spectrum sharing, all operators are allowed to use simultaneously the same frequency resource. However, non-orthogonal spectrum sharing leads to inter-operator interference.</p> <p>To cope with this problem, an efficient approach for dynamic spectrum sharing among co-located Radio Access Networks (RANs) is proposed in this thesis. The basic idea is to partition the available spectrum into private and shared frequency sub-bands. Thus, each operator exclusively uses its private frequency sub-band, while all operators simultaneously utilise the shared frequency sub-band. Those users scheduled in the private frequency sub-band are jointly served implementing multi-cell processing techniques, whereas the rest of the users scheduled in the shared frequency sub-band are served implementing interference coordination among the operators. For this purpose, sparse precoding is applied to minimise inter-operator interference with relying on the exchange of Channel State Information (CSI) among the operators. In addition, a heuristic algorithm based on user grouping is proposed to optimise spectrum partitioning (into private and shared frequency sub-bands) with the aim of maximising the inter-RAN sum rate. Based on simulation results, it is possible to conclude that the proposed dynamic spectrum sharing approach outperforms conventional approaches of allocating exclusive orthogonal sub-bands to operators or sharing the whole available spectrum in a non-orthogonal way.</p>		
Keywords: inter-operator spectrum sharing, non-orthogonal spectrum sharing, RAN, multi-cell processing, interference coordination, sparse precoder, zero-forcing precoder, multi-cell cooperation		

Acknowledgement

This M.Sc. thesis is done as part of Networks of 2020 (NETS2020) project, funded by TEKES, Ericsson, Nokia Siemens Networks, Renesas Mobile Europe, and Nethawk.

First of all, I would like to express my sincere gratitude to my supervisor, Professor Olav Tirkkonen, for giving me the opportunity to work on NETS2020 project, and his guidance and insightful comments during the work. I would like to extend my gratitude to my instructor, Dr. Alexis Dowhuszko, for his constructive comments and guidance during the work.

Last but not least I would like to thank my parents, especially Mulugeta Desta, for their support and love.

Espoo, January 20, 2014.

Sofonias Hailu

Contents

Abstract	ii
Acknowledgement	iii
Contents	iv
1 Introduction	1
1.1 Motivation	1
1.2 Overview of Thesis Problem	2
1.3 Thesis Contribution	3
1.4 Thesis Organization	4
2 Background	5
2.1 Cellular and Heterogeneous Networks	5
2.1.1 Evolution of Cellular Networks	5
2.1.2 Overview of 4G Cellular Networks	6
2.1.3 Heterogeneous Networks	7
2.2 Radio Access Network Architectures	9
2.2.1 Centralised Processing	9
2.2.2 Distributed Processing	10
3 Multi-Cell Cooperation	12
3.1 Conventional Radio Resource Management Approaches in Multi-cell Networks	12
3.1.1 Frequency Reuse	12
3.1.2 Power Control	13
3.1.3 Spreading Code Assignment	13
3.2 Multi-Cell Cooperation Basics	14
3.2.1 Multi-Cell Cooperative Network Architectures	14
3.2.2 Multi-Cell Cooperation Challenges	16
3.3 Multi-Cell Cooperation Techniques	16
3.3.1 Interference Coordination Techniques	16
3.3.2 Multi-Cell Processing Techniques	18
3.3.3 Multi-Cell Cooperation with Limited Backhaul Capacity	20
4 Sparse Precoding	22
4.1 Multicell Joint Transmission Channel	22
4.2 Optimization Criteria	23
4.2.1 Zero-Forcing Criterion	23
4.2.2 Minimizing Mean Square Error (MMSE) criterion	23
4.3 Sparse Precoding based on Sparse Inverse Algorithm	24

5	Dynamic Spectrum Sharing between Co-located RANs	27
5.1	System Model	28
5.1.1	Multi-RAN Joint Transmission Channel	28
5.1.2	System Performance Model	32
5.2	Dynamic Spectrum Sharing	33
5.2.1	Optimisation Problem	33
5.2.2	Heuristic Algorithm based on User Grouping	34
6	Simulation Results and Analysis	37
6.1	Simulation Scenario	37
6.1.1	Network Layout	37
6.1.2	User Distribution	39
6.2	Simulation Parameters and Models	40
6.2.1	Simulation Parameters	40
6.2.2	Antenna Pattern	40
6.2.3	Channel Model	42
6.3	Performance Assessment Method	42
6.4	Comparison of Orthogonal and Full spectrum Allocations	43
6.4.1	User Distribution Type-I	43
6.4.2	User Distribution Type-II	45
6.4.3	User Distribution Type-III	46
6.5	Performance of Dynamic Spectrum Allocation	47
7	Conclusion and Future Work	50
7.1	Conclusion	50
7.2	Future Work	51
	References	52
	Appendices	56
A	Least Squares Problem	56

List of Acronyms

BS	Base Station
CSI	Channel State Information
C-RAN	Centralised processing, Cooperative radio, Cloud, and Clean (Green) Infrastructure RAN
FFR	Fractional Frequency Reuse
ISD	Inter-site Distance
ITU	International Telecommunication Union
LTE	Long Term Evolution
MIMO	Multiple Input Multiple Output
MMSE	Minimizing Mean Square Error
OFDMA	Orthogonal Frequency Division Multiple Access
RAN	Radio Access Network
RRH	Remote Radio Head
SFR	Soft Frequency Reuse
SINR	Signal to Interference Plus Noise Ratio
SNR	Signal to Noise Ratio
UE	User Equipment
3GPP	Third Generation Project Partnership

List of Figures

1	Mobile subscribers growth which is growing rapidly [4]	1
2	Growth of transferred data in Western Europe which is following an exponential growth [5]	2
3	Illustration of multi-carrier principle: A set of overlapping sub-carriers are used for transmission [4]	6
4	Maintaining the sub-carriers' orthogonality: At sampling point for a single sub-carrier, the other sub-carriers have zero amplitude [4] . . .	7
5	Illustration of heterogeneous network showing the co-existence of macro-cell, picocells, relay nodes, Remote Radio Heads (RRHs) and femto-cells [14]. For backhaul connectivity, pico cells use X2 interface, relay nodes use wireless connection, and femtocells use broadband connection.	8
6	Illustration of architecture with a distributed antenna system and a virtual Base Station (BS) pool for central processing [15]. The RRH mainly has radio functionality, and the virtual BS pool has layer 1 and 2 functionalities.	9
7	RAN architecture with distributed self-organising network [5]	11
8	FFR with reuse-1 applied in cell-center and reuse-3 is used in cell-edge, to keep orthogonality among cell-edge users of neighboring cells.	12
9	Multi-cell cooperation with centralised implementation. In this case, the BSs need a central entity to exchange CSI.	14
10	Multi-cell cooperation with distributed implementation. No central entity is required to get global CSI, all User Equipments (UEs) feed their CSI to all BS.	15
11	Comparison of idealized conventional cellular network (top) and coordinated network (bottom) [34]. In the former, a UE can only receive a useful signal from a single BS (treating the signal from other BSs as interference), whereas in the later a UE receives useful signals from all BSs and combines them to boost its received signal quality.	19
12	Principle of multi-cell processing for the downlink [19]. The data intended for a given UE is routed to all BSs and the weight used by each BS is determined based on the global CSI.	20
13	A simple network with a simple data routing where the data symbol for UE 1 is routed to BSs 1 and 2, for UE 2 is routed to BSs 1,2 and 3, and for UE 1 is routed to BS 3.	25
14	Illustration of Dynamic Spectrum Allocation. The total available spectrum is partitioned into private and shared (in a non-orthogonal way) frequency sub-bands in an adaptive way.	27
15	An illustration of co-located RANs. The BSs/RRHs of each RAN are assumed to be connected to a virtual BS pool using fiber optics. Further, the two virtual BS pool are assumed to be connected using fiber optics for the exchange of CSI and signalling information	28

16	Illustration of the simulated network layout. Two co-located Centralised processing, Cooperative radio, Cloud, and Clean (Green) Infrastructure RANs (C-RANs) each consisting of 4 RRHs are considered. The macrocells of each operator share the same towers.	37
17	Illustration of 'User Distribution Type-I'. In this case, a user of an RRH is uniformly distributed within a radius R from the RRH.	38
18	Illustration of 'User Distribution Type-II'. all the users of both operators are uniformly generated within radius R from the center of the RRHs coordinates. The size of R could be large enough to encompass all the RRHs.	39
19	Illustration of 'User Distribution Type-III'. Users of all operators are uniformly generated within radius R from the center of the RRH coordinates. However, users of operator 1 are not allowed to be generated within radius r of operator 2's RRHs, and vice versa.	40
20	Comparison of orthogonal vs full spectrum allocations with user distribution type-I	44
21	Comparison of orthogonal vs full spectrum allocations with user distribution type-II	45
22	Comparison of orthogonal vs full spectrum allocations with user distribution type-III	46
23	Performance of dynamic spectrum allocation is compared with orthogonal and full spectrum allocations under User Distribution Type-I with parameter $R = 60\text{m}$	47
24	Performance of dynamic spectrum allocation is compared with orthogonal and full spectrum allocations under User Distribution Type-II with parameter $R = 65\text{m}$	48
25	Performance of dynamic spectrum allocation is compared with orthogonal and full spectrum allocations under User Distribution Type-III with parameters $R = 65\text{m}$ and $r = 25\text{m}$	49

List of Tables

1	Simulation parameters	41
---	---------------------------------	----

1 Introduction

1.1 Motivation

Driven by the availability of effective network coverage and cheap mobile phones, the number of mobile subscribers has been growing exponentially as shown in Fig. 1. In addition, the introduction of smart phones, tablets, netbooks and cable TV has lead mobile data demand to grow rapidly as shown in Fig. 2. By 2020, the number of mobile subscribers is expected to increase by 10-fold and data usage by 100-fold, when compared to the figures in 2010 [1]. Moreover, 50 billion devices are expected to be connected to the mobile network by 2020, which is expected to boost the demand of mobile data ever since [2].

To cope with the ever increasing mobile traffic demand, a continuous work is being done to increase the capacity of mobile networks. The capacity of mobile networks can generally be improved by increasing the number of Base Stations (BSs), spectral efficiency and operational bandwidth of the network. The introduction of small BSs will play a major role in increasing the number of BSs. In addition, equipping the transmitters and receivers with multiple antennas and enabling multi-cell cooperation between BSs are proved to significantly improve spectral efficiency. Moreover, identifying and using new frequency bands is expected to increase the available spectrum for operators [3].

However, it is difficult to fulfill the expected bandwidth requirement for future mo-

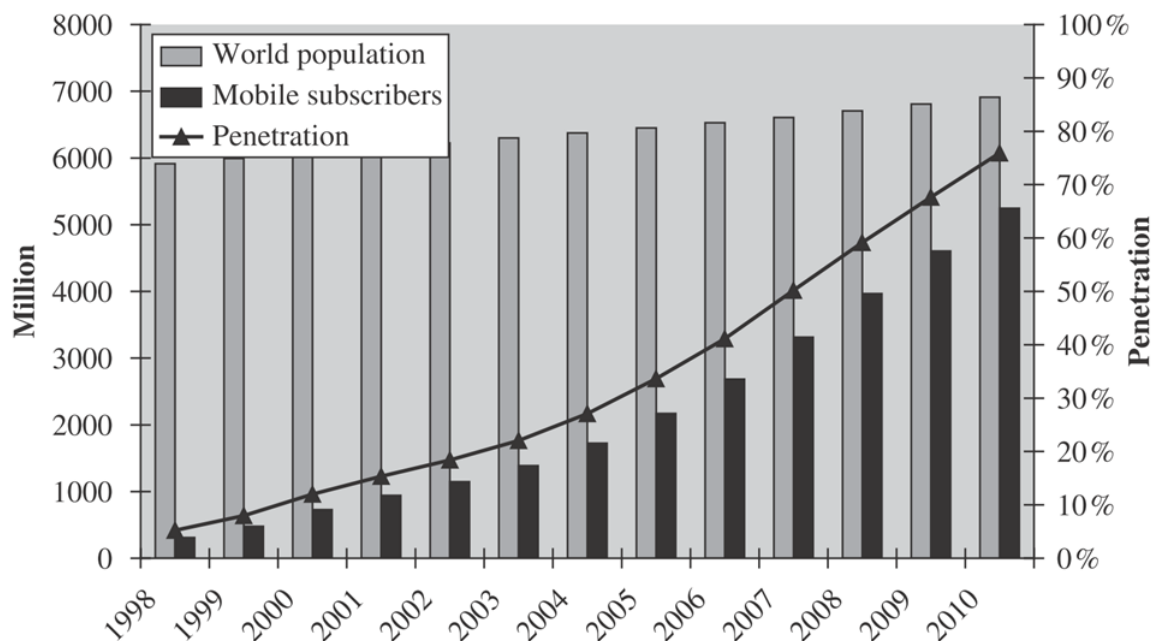


Figure 1: Mobile subscribers growth which is growing rapidly [4]

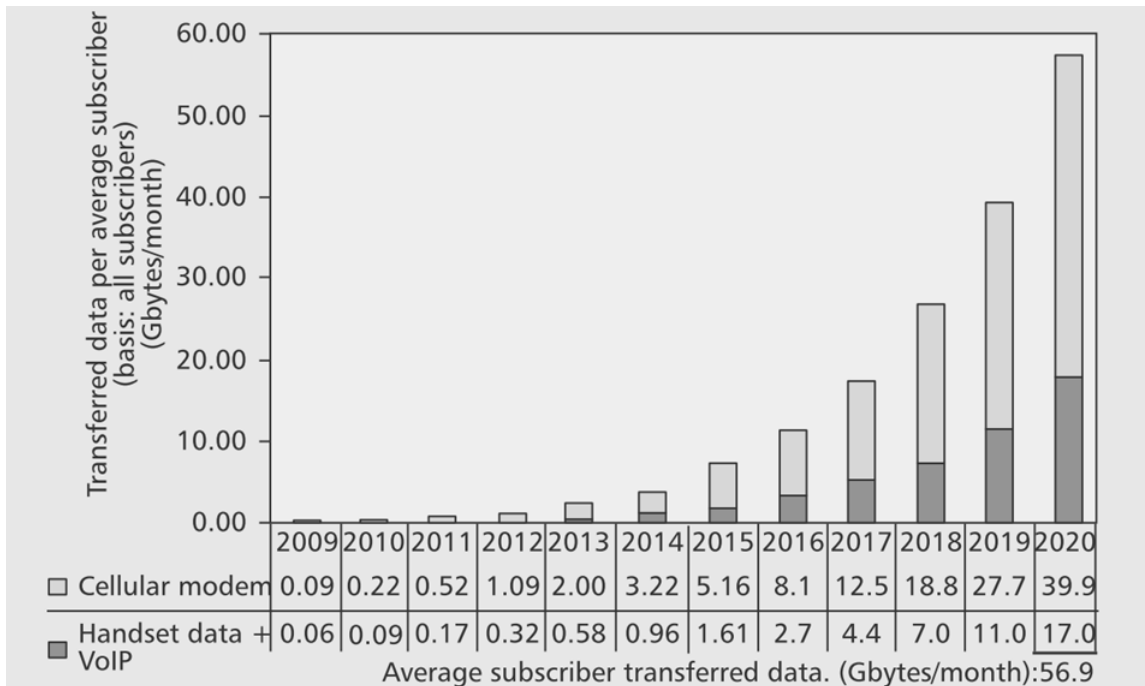


Figure 2: Growth of transferred data in Western Europe which is following an exponential growth [5]

mobile networks if operators make use of dedicated orthogonal frequency sub-bands to operate independently. For example, it is expected that a bandwidth of 1200-1700 MHz will be required in 2020 [6], even though much less bandwidth is yet identified for new usage in the previous world radio conferences (as spectrum below 5GHz is already congested). Due to this, inter-operator spectrum sharing is becoming a viable option for improving operational bandwidth, and is gaining momentum in the research world of telecommunication.

In general, spectrum can be shared in an orthogonal or a non-orthogonal way [7]. In orthogonal spectrum sharing, two operators cannot use the same frequency resource at the same time. As an access method, several game theoretic approaches are used for orthogonal spectrum sharing [8]. In non-orthogonal spectrum sharing, operators simultaneously transmit on the same frequency resource, creating inter-operator interference. In order to minimize the inter-operator interference into a tractable level, transmit beamforming [9] and/or game theoretic [10] approaches are proposed in the literature.

1.2 Overview of Thesis Problem

The problem of adaptively sharing spectrum between co-located Radio Access Networks (RANs) owned by different operators is studied in this thesis. The operators are assumed to be willing to share part of their licensed spectrum in an adaptive

and non-orthogonal way. If we assume the RANs could share full user data and Channel State Information (CSI), then the ideal solution would be to jointly serve all the User Equipments (UEs) of all the RANs in the whole spectrum available for the RANs. However, due to its demand for extremely high capacity and low latency backhaul network, this solution is difficult to implement practically and not considered in this thesis.

We assume the RANs share only CSI and signaling information when adaptively sharing their spectrum. An aggressive approach to share the spectrum could be to share the whole available spectrum by all the RANs in a non-orthogonal way coordinating inter-RAN interference. However, some of the UEs found in the vicinity of other operators' RAN may face strong inter-RAN interference which could be difficult to minimize into a tractable level. A good approach could be to serve the UEs with a strong inter-RAN interference in a private frequency sub-band allocated for exclusive use by their serving RANs, and serve the rest of the UEs in the non-orthogonally shared frequency sub-band. Thus, the spectrum needs to be partitioned into private and shared (in a non-orthogonal way) frequency sub-bands in an optimized adaptive way, and group the UEs to be served in either sub-band.

As an optimization criterion, we consider the maximization of the sum rate of the whole UEs of all the co-located RANs, which we will refer it as inter-RAN sum rate. Therefore, with the aim of maximizing the inter-RAN sum rate, the combined problem of partitioning the spectrum in to private and shared frequency sub-bands and scheduling the UEs in either sub-band is studied in this thesis. Besides, the problem of adaptively partitioning the spectrum is also analyzed in order to take into account the location and channel condition of the UEs.

1.3 Thesis Contribution

In this thesis, an efficient approach is proposed for adaptive inter-operator spectrum sharing among co-located RANs owned by different operators. Rather than sharing a fixed amount of spectrum and concentrate on how to minimize the inter-RANs interference, we allow the amount of shared spectrum to be variable, taking into account the location and channel condition of the UEs. In other words, the proposed approach enables operators to adaptively share part of their spectrum non-orthogonally, while keeping the unshared spectrum portion for their private use.

A heuristic algorithm based on user grouping is proposed for the purpose adaptively partitioning the available spectrum into private and shared frequency sub-bands, with the aim of maximizing the inter-RANs sum rate. The algorithm takes into account the location and channel condition of the UEs, and the applied mechanism for inter-RAN interference minimization. As a tool for minimizing the inter-RAN interference, Sparse precoding [11] is used as an inter-RAN precoder. Sparse precoding is originally used as a multicell processing approach, for jointly serving UEs where the amount of user data shared is limited.

1.4 Thesis Organization

The next chapters are summarized as follows. Chapter 2 briefly reviews cellular and heterogeneous networks, and RAN architectures.

In Chapter 3, multi-cell cooperation is discussed. First, the conventional radio resource management approaches are briefly introduced. Then, the architectures and challenges in multi-cell cooperation are briefly explained. This is followed by the presentation of the two broad categories of multi-cell cooperation techniques, namely interference coordination techniques and multi-cell processing techniques. Finally, multi-cell cooperation techniques with limited backhaul capacity are briefly discussed.

In Chapter 4, sparse precoding is covered. Sparse precoding is a multi-cell cooperation technique which is originally used for networks with limited data sharing capability. The multicell joint transmission channel used for explaining the scheme is briefly revised along its optimization criteria before presenting the algorithm in more detail.

In chapter 5, the proposed adaptive inter-operator spectrum sharing approach is explained. First, the system model is presented. The optimization problem is then formulated. Finally, a heuristic algorithm based on user grouping is explained, which is used for adaptively sharing the spectrum among the RANs of different operators.

In chapter 6, simulation results are presented and analyzed. The simulation scenario, simulation parameters, user distributions and channel models are first explained. The performance of orthogonal and full spectrum allocations are then compared and discussed. The performance of the proposed adaptive spectrum sharing approach is then compared with orthogonal and full spectrum allocation approaches, and results are discussed. In the last chapter, conclusions are drawn and further potential future works are suggested.

2 Background

2.1 Cellular and Heterogeneous Networks

A cellular network is a wireless communication system through which UEs are able to communicate with each other and access other networks, such as the internet and the public switched telephone network, throughout a wide range of geographical area. It consists of RAN and core network. The RAN consists of UEs, BSs and network entities which control and coordinate the BSs, such as Base Station Controllers (BSCs) in Global System for Mobile (GSM) and Radio Access Controllers (RNCs) in Wideband Code Division Multiple Access (WCDMA). Since it is not possible to serve a wide range of geographical area with a single radio transceiver, it is divided into small service areas called cells. In each cell, there is always a BS which provides the necessary radio interface operations for the UEs located in the cell.

Unlike RAN, the core network serves as a switching center and gateway to other networks such as the internet and public switched telephone network. It provides services related to authentication, billing, mobility and roaming. Several interfaces exist in order to interconnect the network entities in RAN and core network. For example, the UEs are connected to the BSs through an air interface, and RAN to the core network through a wired or a wireless interface.

2.1.1 Evolution of Cellular Networks

The cellular network has made several evolution and is still evolving. The first cellular networks, called 1st Generation (1G) networks, were analogue, insecure and less efficient systems. Nordic mobile telephony system and the advanced mobile phone service can be taken as an examples of 1G network. In the following generation of cellular networks, called 2nd generation (2G) networks, a digital, secure and efficient system was developed, and short message sending and low rate data services were introduced. The widely deployed GSM and Interim Standard 95 (IS-95) are among the 2G networks. The introduction of packet core network improves the data rate of 2G networks. This paved the way for 3rd generation (3G) networks. However, the 2G networks did not directly evolved to 3G. Instead, GSM First Evolved to General Packet Radio Service (GPRS) and Enhanced Data Rates for GSM Evolution (EDGE), which are sometimes referred as 2.5G and 2.75G, respectively, before it finally evolved to WCDMA, a 3G network. Similarly, IS-95 evolved to 1 Times Radio Transmission Technology (1xRTT) before it evolved to Code Division Multiple Access 2000 (CDMA2000).

The 3G networks were developed in accordance with International Telecommunication Union (ITU) specifications, called International Mobile Telecommunications-2000 (ITU-2000) standard. The Universal Mobile Telecommunications System (UMTS), which was proposed by Third Generation Project Partnership (3GPP), CDMA2000 and Worldwide Interoperability for Microwave Access (WiMAX) are among the

cellular technologies which comply with ITU-2000 standards and provide relative higher data rates. Several improvements were made to 3G networks before they finally evolved towards 4th generation (4G) networks. For example, the 3GPP's WCDMA evolved to High Speed Packet Access (HSPA), HSPA+ and Long Term Evolution (LTE), which are considered as 3.5G, 3.75G and 3.9G, respectively, before it finally evolved to 4G. Currently, LTE-Advanced and WiMAX, which are developed by 3GPP and the Institute of Electrical and Electronics Engineers (IEEE), respectively, are considered as 4G technologies. These technologies are not deployed yet, but they are expected to provide very high data rates.

2.1.2 Overview of 4G Cellular Networks

Several proposals were submitted as a response to the ITU's circularly letter for proposal for technologies which comply with IMT-Advanced standard [12]. Among the submitted technologies, the 3GPP's LTE-Advanced and IEEE's WiMAX, which is also referred as IEEE 802.16e, were accepted as technologies which fulfill the requirements for IMT-Advanced. LTE-Advanced even surpass some of the requirements. Among the requirements for IMT-Advanced include [13]:

- Peak spectral efficiency of upto 15 bits/s/Hz in the downlink and 6.75 bits/s/Hz in the uplink;
- A downlink peak data rate of 1 Gbps for stationary users;
- A user plane latency of 10 ms;

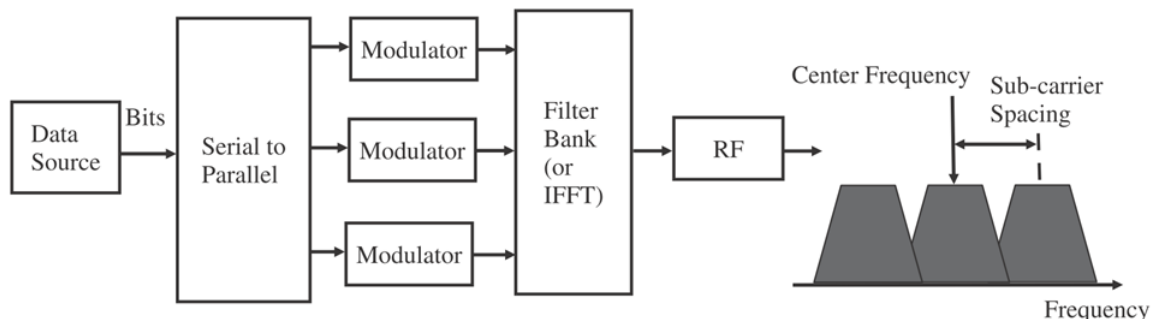


Figure 3: Illustration of multi-carrier principle: A set of overlapping sub-carriers are used for transmission [4]

On the other hand, these technologies use Orthogonal Frequency Division Multiple Access (OFDMA) for their air interface. OFDMA is a multi-carrier modulation scheme, where the data to be transmitted is divided into parallel data streams, and each data stream modulates a distinct sub-carrier from a set of sub-carriers as shown in Fig. 3. The sub-carriers are allowed to overlap, while keeping their orthogonality. As shown in Fig. 4, the orthogonality is maintained by adjusting the system parameters such that during the sampling period of each sub-carrier, other sub-carriers

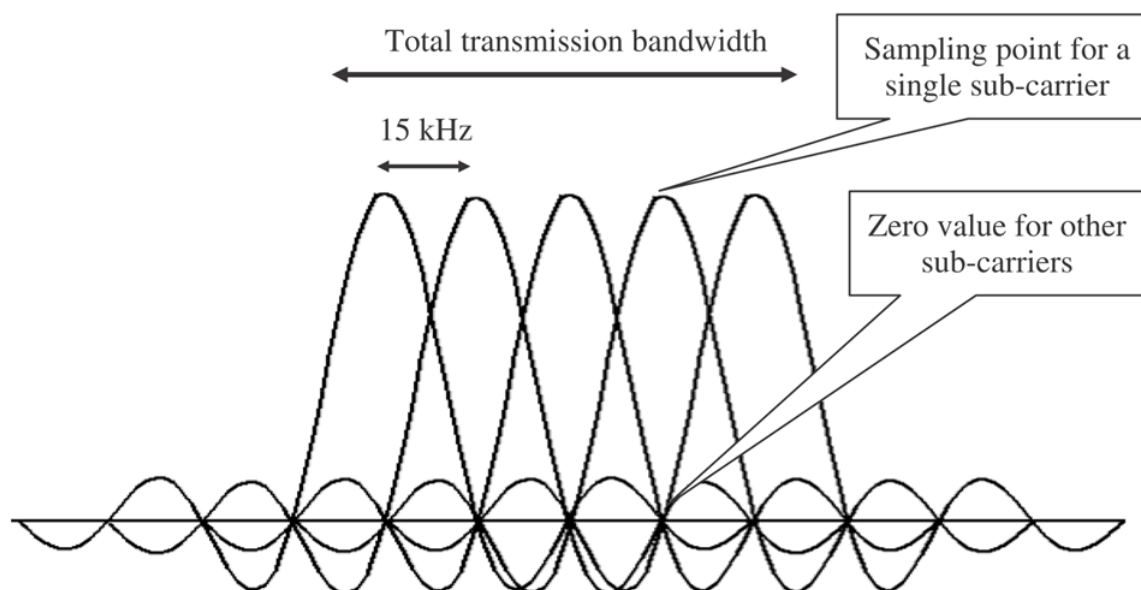


Figure 4: Maintaining the sub-carriers' orthogonality: At sampling point for a single sub-carrier, the other sub-carriers have zero amplitude [4]

have zero amplitude.

As listed in [4], among the interesting properties of OFDMA, it can be listed the following abilities:

- good performance in frequency selective fading;
- low complexity of base-band receiver;
- good spectral properties and handling of multiple bandwidth;
- link adaptation and frequency domain scheduling;
- compatibility with advanced receiver and antenna technologies;

In addition, both technologies employ an enhanced Multiple Input Multiple Output (MIMO) system, which is important for improving spectral efficiency and signal quality. Besides to this, LTE-Advanced introduces technologies like carrier aggregation and relaying. In carrier aggregation, carriers of previous releases of LTE are aggregated to achieve higher bandwidth, at the same time keeping backward compatibility. The aggregated carriers can be either from a contiguous bandwidth (intra-band) or a non-contiguous bandwidth (inter-band).

2.1.3 Heterogeneous Networks

As the cellular networks evolve, they are becoming more heterogeneous, with several types of BS deployed together. The main reason to carry out an heterogeneous

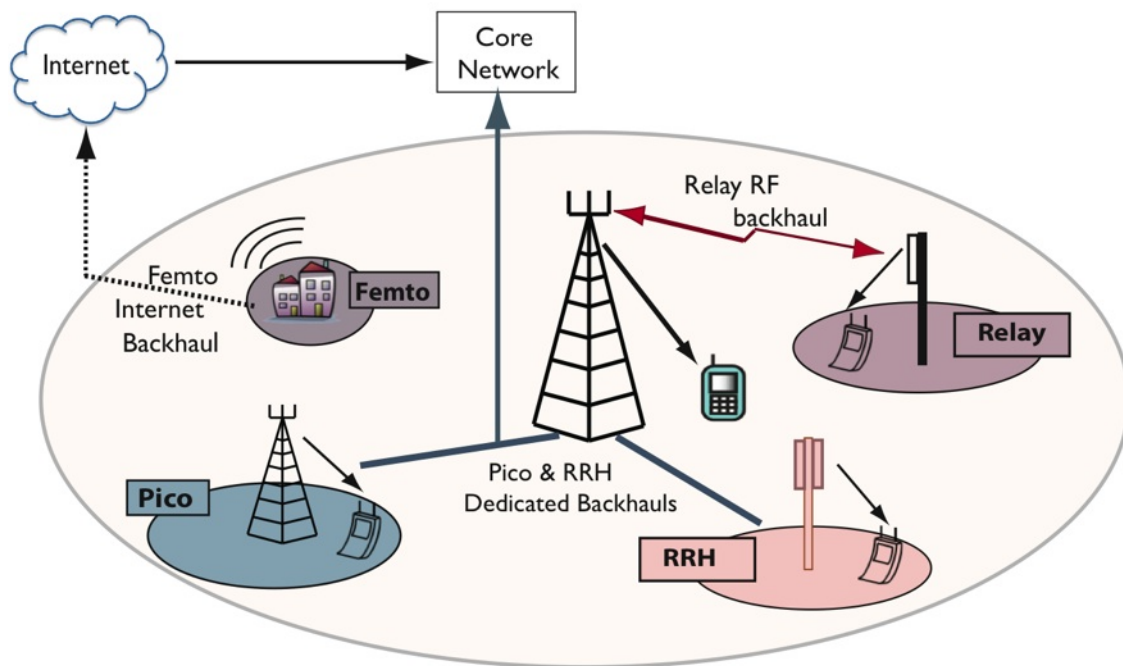


Figure 5: Illustration of heterogeneous network showing the co-existence of macro-cell, picocells, relay nodes, RRHs and femtocells [14]. For backhaul connectivity, pico cells use X2 interface, relay nodes use wireless connection, and femtocells use broadband connection.

network deployment is to increase the area spectral efficiency, so that optimal user experience is provided throughout the coverage area. For this reason, the deployment of the macro BS, which provides the basic coverage, is accompanied by the deployment of picocells, RRHs, relay nodes and femtocells as shown in Fig. 5.

Pico cells are low power nodes, which are deployed by the operator in hotspot areas, and areas with coverage hole. They are connected to the macrocell through the X2 interface. Similarly, relay nodes are also low power nodes, which are wirelessly connected to the macrocell. They are deployed by the operator in remote areas with difficulties for having wireline backhaul, and areas with weak signal power such as cell edge and tunnels. On the other hand, RRH are a compact sized and low weight units, which are connected to the conventional BS through fiber optics to form a distributed antenna system. They are used to provide coverage to remote areas, and areas with site acquisition problems. Finally, femtocells are small access points which are deployed by users. They are suitable for home and enterprise uses, and mainly operate in closed subscriber group mode. They use the broadband connection of the user for backhaul connectivity, which makes this deployment simple.

2.2 Radio Access Network Architectures

The traditional RAN architecture consists of a set of BSs, where a fixed number of sector antennas are connected to each BS. Each antenna independently covers its coverage area and handles only the signals to and from its own UEs. However, due to several reasons, such architecture is inefficient for future networks, which mainly will be heterogeneous in nature [15]. One of the reasons is that traditional RAN is not suitable for centralized interference management, where sometimes cooperative transmission and reception, and interference coordination is required. Another reason is that its difficulty to incorporate new services, which could potentially increase the revenue of operators. Due to these factors, two types of RAN architectures based on the available backhaul network capacity are considered for future networks. The RAN architectures are differentiated based on their centralized or distributed processing system [5].

2.2.1 Centralised Processing

The wireline capacity is increasing rapidly with the advancements experienced in the

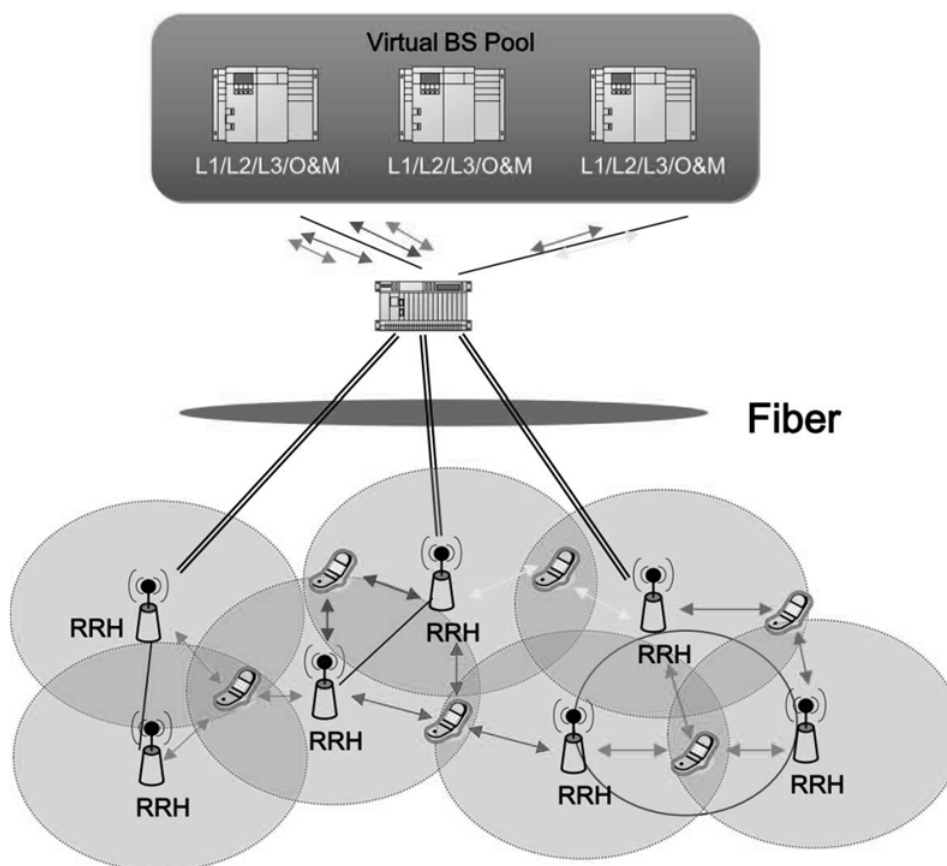


Figure 6: Illustration of architecture with a distributed antenna system and a virtual BS pool for central processing [15]. The RRH mainly has radio functionality, and the virtual BS pool has layer 1 and 2 functionalities.

field of fiber optics. The introduction of Wavelength-Division Multiplexed Passive Optical Network (WDM-PON) is expected to further enhance the capacity of passive optical networks (PON) [16]. Besides to this, ultra-wide band microwave is also expected to be an additional option for backhaul connectivity. On the other hand, the computing capacity is increasing rapidly according to Moore's law. Therefore, with the expected popularity of WDM-based access networks in the near future, a RAN architecture with centralizing processing is expected to be among the popular RAN architectures for future cellular networks.

One of such architectures known as Centralised processing, Cooperative radio, Cloud, and Clean (Green) Infrastructure RAN (C-RAN) is proposed by China Mobile Research Institute. The C-RAN architecture consists of a baseband unit and a distributed antenna system with RRH, as shown in Fig. 6. There are two ways of implementing C-RAN [15]. The first solution is a fully centralized approach, where the baseband unit has all the functionalities of layer 1, layer 2 and layer 3, and the RRH have only the radio functionality. In the second solution, a partially centralized approach is applied where the baseband unit has the functionalities of layer 2 and layer 3, whereas the RRH includes layer 1 functionality in addition to the radio functionality.

In general, C-RAN architecture has several advantages when compared to the traditional RAN architecture [15]. First of all, it is energy efficient and represents an eco-friendly infrastructure. Secondly, it leads to lower Capital Expenditure (CAPEX) and Operational Expenditure (OPEX). The third advantage of C-RAN architecture is its suitability for multi-cell cooperation as signaling information, user data and CSI can be easily shared among the baseband units. This significantly improves the system capacity. The other advantages of C-RAN architecture are its capability for adapting to non-uniform traffic, and using intelligent devices in the C-RAN to offload internet traffic from smart phones and devices.

2.2.2 Distributed Processing

In RAN architectures with distributed processing, some of the RAN functionalities are distributed in the BSs, or small access points. Such architecture is useful for large networks, or networks with expensive backhaul. For this reason, distributed Self Organizing Network (SON), which is a typical example of RAN architecture with distributed processing, is expected to be one of the dominant RAN architectures of the future network, especially those scenarios which have a large number of small cells. As shown in Fig. 7, the small access points are able to communicate with each other, and they have the functionality of SON such as self-configuration, self-organization, and self-healing [5].

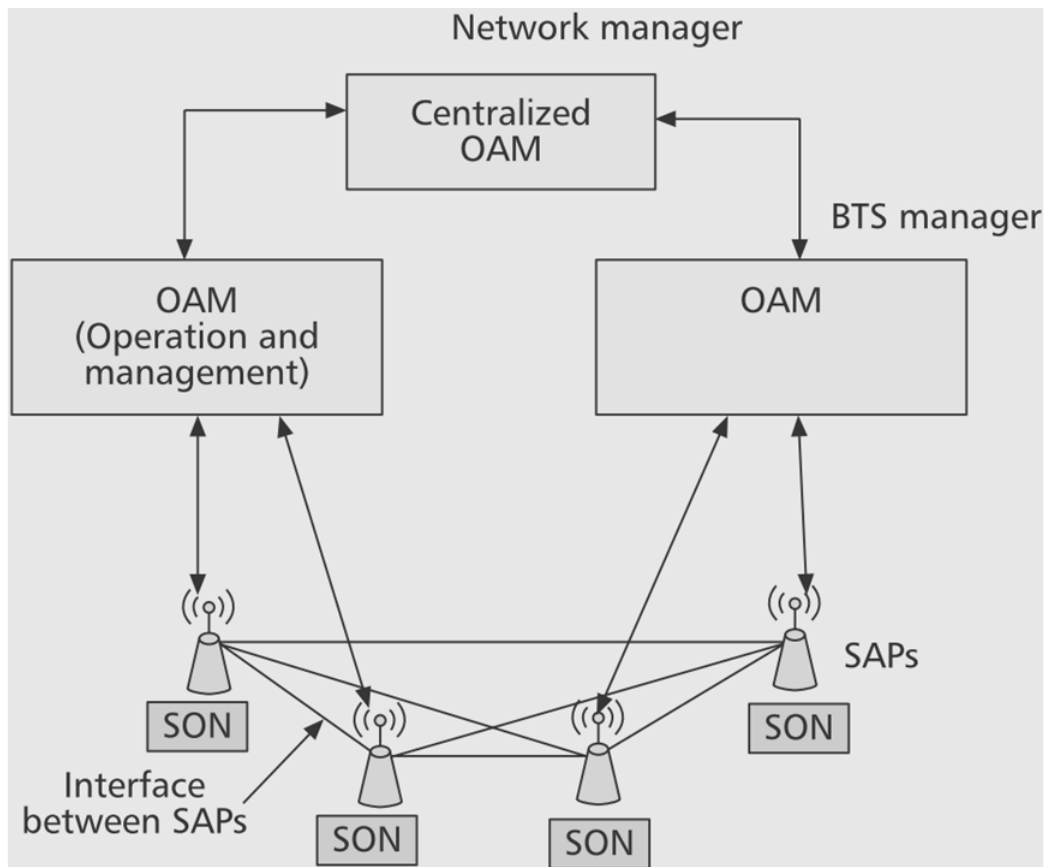


Figure 7: RAN architecture with distributed self-organising network [5]

3 Multi-Cell Cooperation

In multi-cell networks, radio resources are reused for efficient utilization of the available resources. However, this leads to inter-cell interference, which needs to be properly managed in order to get the required performance improvements. Conventional radio resource management approaches include frequency reuse, power control, and spreading code assignments [17, 18]. On the other hand, several papers have extended the MIMO transmission techniques for multi-cell cooperation. These techniques can be classified as multi-cell interference coordination and multi-cell processing techniques [19]. In general, Multi-cell cooperation techniques can significantly reduce the inter-cell interference and improve the spectral efficiency.

3.1 Conventional Radio Resource Management Approaches in Multi-cell Networks

3.1.1 Frequency Reuse

Since spectrum is scarce and expensive, every operator tries to reuse its spectrum as much as possible to improve its capacity without too much degradation of the performance of cell edge users. For this reason, several frequency reuse strategies are used. Among the common frequency reuse strategies include reuse- n , Fractional Frequency Reuse (FFR) and Soft Frequency Reuse (SFR) [20, 21, 22]. Reuse- n is the simplest frequency reuse pattern when $n > 1$, the inter-cell interference from neighboring cells can be avoided. Even though we can significantly reduce the inter-cell interference and improve the signal quality, such reuse scheme leads to a poor utilization of the available spectrum especially for higher reuse factor.

Unlike Reuse- n , FFR tries to use the spectrum more efficiently. In FFR, the fre-

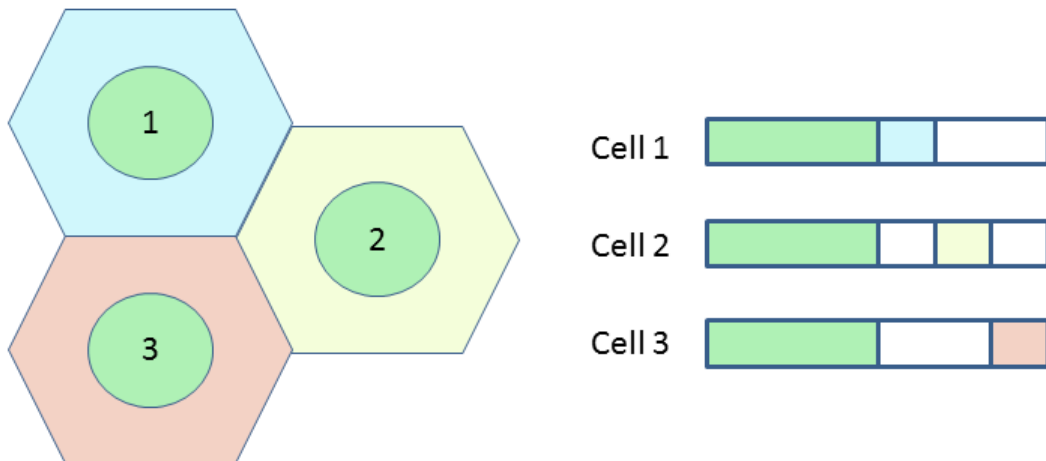


Figure 8: FFR with reuse-1 applied in cell-center and reuse-3 is used in cell-edge, to keep orthogonality among cell-edge users of neighboring cells.

frequency is partitioned into two parts, which are used by cell-center and cell-edge users. The frequency band for the cell-center users generally has a smaller frequency reuse factor than the one for the cell-edge users. One example of FFR configuration is to use the frequency for cell-center users with Reuse-1, and the frequency for cell-edge users with Reuse-3, see Fig 8 for more details. With such configuration, the orthogonality of the frequency assigned to neighboring cell-edge users can be kept, while at the same time providing higher frequency reuse factor for cell center users which are generally less vulnerable to inter-cell interference. In SFR, a more aggressive approach than FFR is used, by allowing the frequency assigned for cell-edge users to be reused by cell-center users of the neighboring cells. This leads for the cell-edge users to face interference from the neighboring cells. One of the approaches used to minimize the interference to the cell-edge users is to serve the cell-center users with less power than the cell-edge users.

Several papers have generally shown that the performance of FFR and SFR can be improved by allowing coordination between neighbouring BSs. To mention a few, in [21], a dynamic FFR based on graph theory is proposed. Based on simulation results, the proposed scheme provides a notable performance improvement over the conventional FFR. Similarly, in [22], a generalised FFR is proposed, which takes into account the irregularity of the shape of cells in the real cellular systems. This scheme provides a significant throughput improvement, as shown by simulation results.

3.1.2 Power Control

Power control plays an important role for mitigating inter-cell interference if the same frequency is reused in neighbouring cells. As seen in the previous subsection, power control is used to mitigate the inter-cell interference to neighbouring cell-edge users in SFR. In addition, power control plays an important role to mitigate the inter-cell interference in Code Division Multiple Access (CDMA) systems, where frequency Reuse-1 is applied. In CDMA, a tight power control is used, as the system is more prone to intra- and inter-cell interference due to its sensitiveness to the received power difference in the BS. When a user is found in the border of cells, power control is applied in conjunction with soft handover to keep the required level of received signal power for the user, without disturbing other users.

3.1.3 Spreading Code Assignment

In this radio resource management approach, the receiver treats the inter-cell interference as noise, and tries to indirectly mitigate the inter-cell interference by improving its link level performance using spreading code assignments and/or MIMO techniques [17, 23]. When a spreading code is used, for example, in systems which use spreading spectrum technology, the interference is systematically averaged over a wide band. More over, with the application of multiple antennas in the transmitter and/or receiver, transmit and/or receive diversity can be applied to combine the signals to be transmitted and/or received, in order to improve the link level performance.

3.2 Multi-Cell Cooperation Basics

The conventional radio resource techniques that we have seen in the previous section are done with no or little coordination between the BSs. When there is a coordination, it is mainly in the form of scheduling, user assignment, or soft hand over techniques. Besides, some of them are done in a static way. On the contrary, in multi-cell cooperation, BSs coordinate their usage of power, time slot, sub-carrier, beamforming coefficients, and other physical and link layer parameters, with the exchange of global CSI. In addition, data symbols can be shared among the BSs, they can also cooperatively code and decode the signals to be transmitted and received. Techniques pertaining to the former are classified as interference coordination techniques, while one belonging to the later as known as multi-cell processing techniques [19]. In such systems, a backhaul network with very low latency and high capacity is generally required.

3.2.1 Multi-Cell Cooperative Network Architectures

Global CSI is generally required for multi-cell cooperation. There are two ways of sharing the CSI, which are used in centralized and distributed architectures [24, 25].

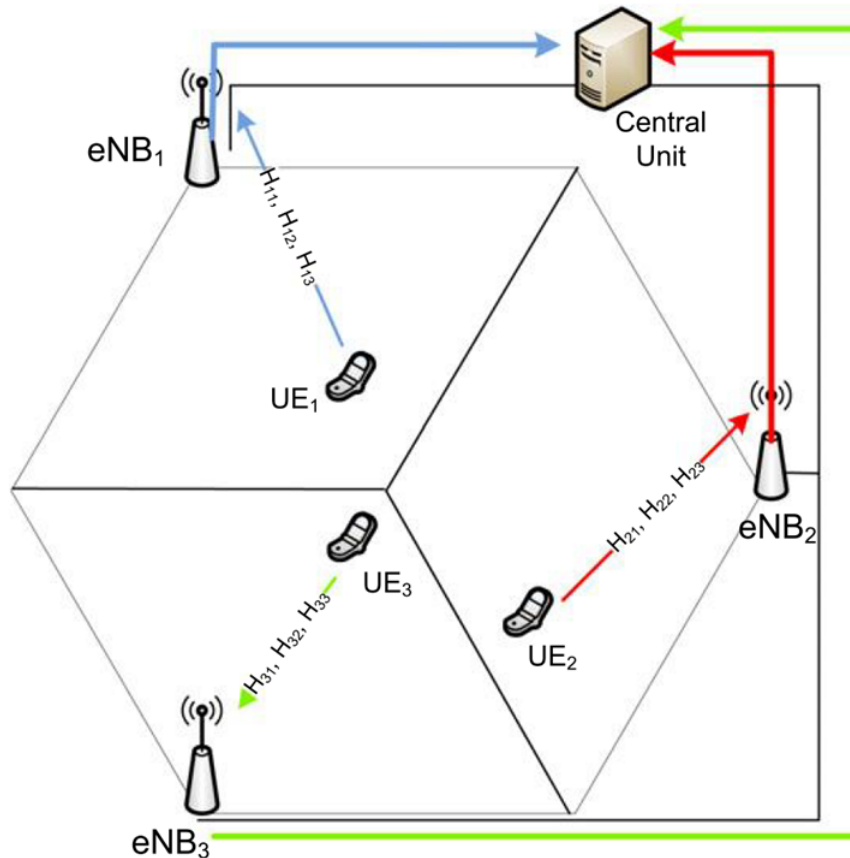


Figure 9: Multi-cell cooperation with centralised implementation. In this case, the BSs need a central entity to exchange CSI.

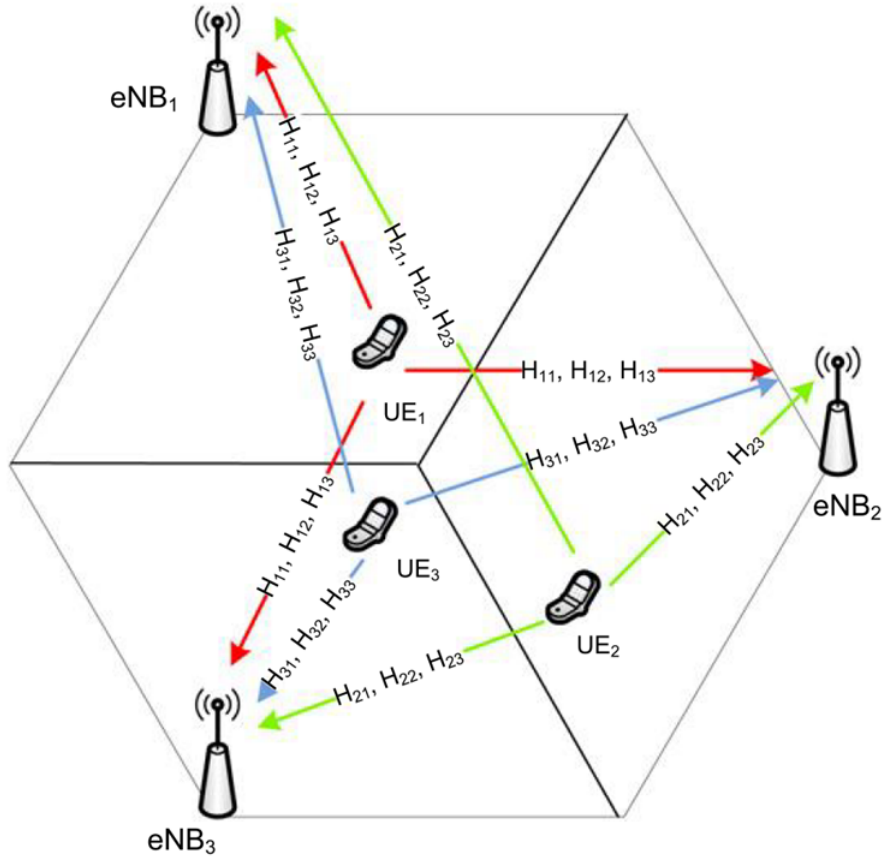


Figure 10: Multi-cell cooperation with distributed implementation. No central entity is required to get global CSI, all UEs feed their CSI to all BS.

In centralized architecture, each UE feeds its channel estimates to a central entity as shown in Fig. 6a. The central entity then performs interference coordination or multi-cell processing operations, based the collected global CSI. One of the challenges for this architecture is the requirement for low-latency high-capacity backhaul links.

On the other hand, in distributed architecture, rather than a centralized entity, identical schedulers are used in each BS. Each UE feeds its channel estimates to all BSs in the cooperative area. Therefore, each scheduler will have the same global CSI to run the algorithm for interference coordination or multi-cell processing independently. Since each scheduler is assumed to be identical, they produce similar results after running the algorithm. However, some of the links might be highly vulnerable to errors, especially those to the BSs found far away. This may result in different global CSI to be received by the schedulers, which results in an overall performance degradation.

3.2.2 Multi-Cell Cooperation Challenges

There are several challenges associated with multi-cell cooperative transmission [24]. One of the challenges is related to channel estimation capability of UEs, and the corresponding requirement for feedback. It is especially challenging for a UE to estimate the channel to the BSs found far away. In addition, providing enhanced feedback in Frequency Division Duplex (FDD) systems introduces additional signalling overhead, which reduces the uplink capacity and increases the mobile terminal battery consumption. Moreover, providing low-latency and high-capacity link for the signal and user data exchange is challenging.

Even though providing solutions for the above challenges is still a hot research area, several papers propose solutions for some of these challenges. In [26], they proposed a scheme which works with reduced CSI by omitting the weak channels. This scheme works as a trade of to performance. In addition, several papers exist which deal with applying multi-cell cooperation with limited backhaul capacity, e.g., [27, 28].

3.3 Multi-Cell Cooperation Techniques

3.3.1 Interference Coordination Techniques

Interference coordination techniques can be applied if we have limited backhaul capacity to support the exchange of user data. However, the backhaul still need to have a very low latency to enable the exchange of global channel information, i.e., of both the direct and the interfering channels, and other signalling information required for coordination among the BSs. Among the commonly applied multi-cell interference coordination techniques include coordinated scheduling, coordinated power control, coordinated beamforming and coding for interference mitigation. Since coordinated scheduling is mostly applied in conjunction with the other techniques, we only briefly review the other three interference coordination techniques as follows:

Coordinated power control

The 4G and beyond cellular networks mainly operate with full frequency reuse. In addition, due to the densely deployed networks and heterogeneous networks, their topology is expected to have a significantly overlapping cells. In such interference limited networks, joint power control and scheduling plays an important role in mitigating the inter-cell interference and improving their performance. But, the problem of joint power control and scheduling is generally challenging. In order to express the problem formally, lets consider an OFDMA based multi-cell network where each cell has multiple UEs. If each UE is scheduled on a separate frequency, the problem includes how the UEs to be scheduled are selected, and how to allocate the power per each sub-carrier to optimize a given performance metric, such as the sum rate of UEs.

If, as an example, we consider the maximization of the sum of the weighted sum of the rate of the UEs, the optimization problem can be mathematically expressed as

follows [19]

$$\begin{aligned} \max \quad & \sum_{l=1}^M \sum_{k=1}^K \alpha_{lk} R_{lk} \\ \text{s.t.} \quad & R_{lk} = \sum_{n \in N_{lk}} \log_2 \left(1 + \frac{P_l^n |h_{l,l,k}^n|^2}{\sum_{j \neq l} P_l^n |h_{j,l,k}^n|^2 + 1} \right) \end{aligned} \quad (1)$$

where M cells each having K number of UEs and N sub-carriers are considered. In addition, the channel from the l^{th} BS to the k^{th} UE in the l^{th} cell on sub-carrier n is denoted as $h_{l,m,k}^n$. Moreover, the power allocated to the n^{th} sub-carrier in the l^{th} BS is denoted by P_l^n , the set of frequencies which are scheduled for the k^{th} UE in the l^{th} cell is denoted as N_{lk} , and the priority of each UE is included in α_{lk} .

Several approaches are applied to solve the above optimization problem. To mention a few, in [29], an iterative algorithm which iterates between the power allocation, which is done cooperatively, and the scheduling, which is done locally, is used to give a sub optimal solution for the optimization problem. Game theoretic approach where each cell independently tries to optimize its power usage, is also an approach used to solve the problem [30]. Another interesting approach uses the idea of interference pricing, where each BS exchanges the measure of the impact of its transmission on UEs found in other cells [31]. Based on the exchanged information, each BS tries to optimize its power allocation.

Coordinated beamforming

If the BSs have multiple antennas, they can have more than one spatial dimension. In addition, if the UEs have less number of antennas than the BSs, the BSs could have additional spatial dimensions, which could be used to minimize the inter-cell interference. We can even completely null the inter-cell interference if the number of additional spatial dimensions that each BS has is greater than the number of dominant interference. Therefore, with the exchange of the global channel information, the BSs can coordinate their beamforming vectors to optimize a given performance metric such as fulfilling a minimum set of Signal to Interference Plus Noise Ratio (SINR) targets, or improving the overall performance.

However, the optimization problem is non-convex in nature, which makes it difficult to solve. In addition, since BSs usually have many UEs, the incorporation of user scheduling into the problem makes it even more complicated. By formulating the optimization problem as the minimization of a function of the transmit power across the BS with a constraint on the SINR of the UEs, a global optimum solution could, however, be found [19, 32]. Mathematically, the optimization problem is expressed as follows [32]

$$\begin{aligned} \min \quad & \sum_{i,j} \mathbf{w}_{i,j}^H \mathbf{w}_{i,j} \\ \text{s.t.} \quad & \mathbf{\Gamma}_{i,j} \geq \gamma_{i,j}, \forall i = 1 \cdots N, j = 1 \cdots K \end{aligned} \quad (2)$$

where we considered a system with N cells each having K UEs with single antenna and a BS equipped with N_t antennas. In addition, the transmit beamforming vector for the j^{th} UE in the i^{th} cell is denoted by $\mathbf{w}_{i,j}$. Moreover, the SINR of the j^{th} UE in the i^{th} cell which is denoted as $\Gamma_{i,j}$ is given as:

$$\Gamma_{i,j} = \frac{|\mathbf{w}_{i,j}^H \mathbf{h}_{i,i,j}|^2}{\sum_{l \neq j} |\mathbf{w}_{i,l}^H \mathbf{h}_{i,i,j}|^2 + \sum_{m \neq i,n} |\mathbf{w}_{m,n}^H \mathbf{h}_{m,i,j}|^2 + \sigma^2} \quad (3)$$

where the channel from the BS of the l^{th} cell to the j^{th} UE in the i^{th} cell is denoted as $\mathbf{h}_{i,i,j} \in \mathbb{C}^{N_t \times 1}$, and the noise is assumed to have a circularly symmetric complex Gaussian distribution with variance σ^2 . In (3), the first term of the denominator represents the intra-cell interference, while the second term the inter-cell interference.

The authors of [32] use a generalised uplink-downlink duality to propose an algorithm based on an iterative function evaluation, to solve the above minimization problem. The algorithm leads to global optimum, and it can be implemented distributively in Time Division Duplex (TDD) systems.

Coding for interference mitigation

The interference signal is generally too weak to detect by out-of-cell UEs. However, if it could somehow be detected, the overall performance of UEs could further be improved by interference cancellation. In [33], the overall performance improvement of UEs with single antenna in a multi-cell environment, where the BSs are equipped with multiple antennas is studied with the use of decodable interference signals. In the paper, the authors use the previously renowned interference decoding approach based on splitting the message into two parts, a common message which can be decoded by all UEs, and a private message which can be decoded by specific UEs only. Therefore, the rate is split into low rate part and high rate part, and the problem of determining UEs in adjacent cells for cell-rate splitting and finding the optimal beamforming vector is jointly solved. According to the simulation results, a significant overall performance improvement can be achieved with this method.

3.3.2 Multi-Cell Processing Techniques

As we have seen in the the interference management techniques explained in the previous sections, the signal which comes from the non-serving cells is always treated as noise, and the network is interference limited. However, if we could share the users data among the BSs in addition to the CSI, every signal arriving at each receiver will no longer be an interference but rather a useful signal, which can be combined to boost the capacity of the system, as shown in Fig. 11. However, a high capacity and very low latency backhaul is required, in order to share the CSI and the user data as shown in Fig. 12.

Assuming we have the required backhaul requirement, how the BSs should coordinate for multi-cell processing is the central question which is widely studied in

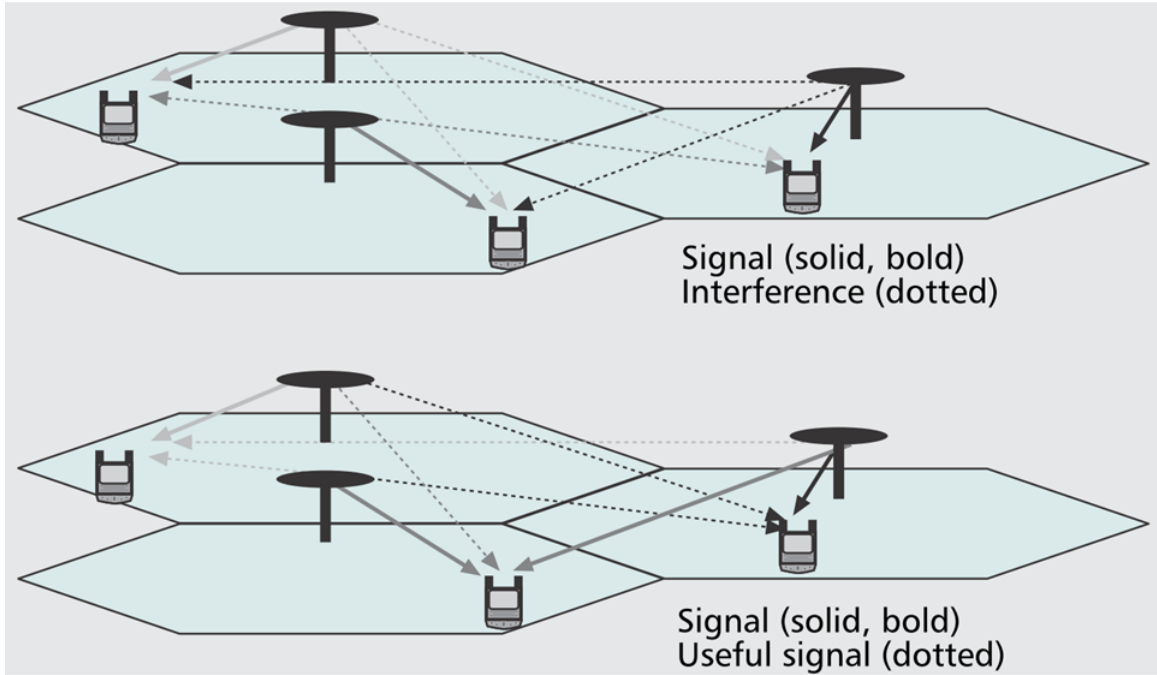


Figure 11: Comparison of idealized conventional cellular network (top) and coordinated network (bottom) [34]. In the former, a UE can only receive a useful signal from a single BS (treating the signal from other BSs as interference), whereas in the later a UE receives useful signals from all BSs and combines them to boost its received signal quality.

the literature. In order to adopt the well developed MIMO-techniques, many papers model the multi-cell cooperation as a virtual MIMO system, where the BSs are considered as spatially distributed antenna arrays. In [34, 35, 36], the popular dirty paper coding scheme is extended to multi-cell cooperation where it is applied in combination, with a linear precoding. In addition, other multi-cell cooperation approaches, such as Tomlinson-Harashima precoding [37], and multi-user detection in MSs [38] can be applied for BS cooperation. However, even though all these non-linear approaches can provide significant performance improvement, they are difficult to implement due to the complexity of the requirements on both the BSs and UEs. Due to this, several linear precoding approaches, which are easier to implemented, are proposed in the literature.

In linear precoding, the BSs jointly optimize the precoding matrix based on one of the optimization metrics, such as minimization of the mean square error (MSE) [39], maximization of the signal to leakage ration plus noise ration (SLNR) [40], and maximization of the sum rate [35, 41]. In minimization of the total MSE, the transmitter precoders are optimized to minimize the sum of the MSEs between the received signal and the desired signal, which would be obtained in a single multi-user MIMO environment without multi-user interference and noise. On the other hand, in the

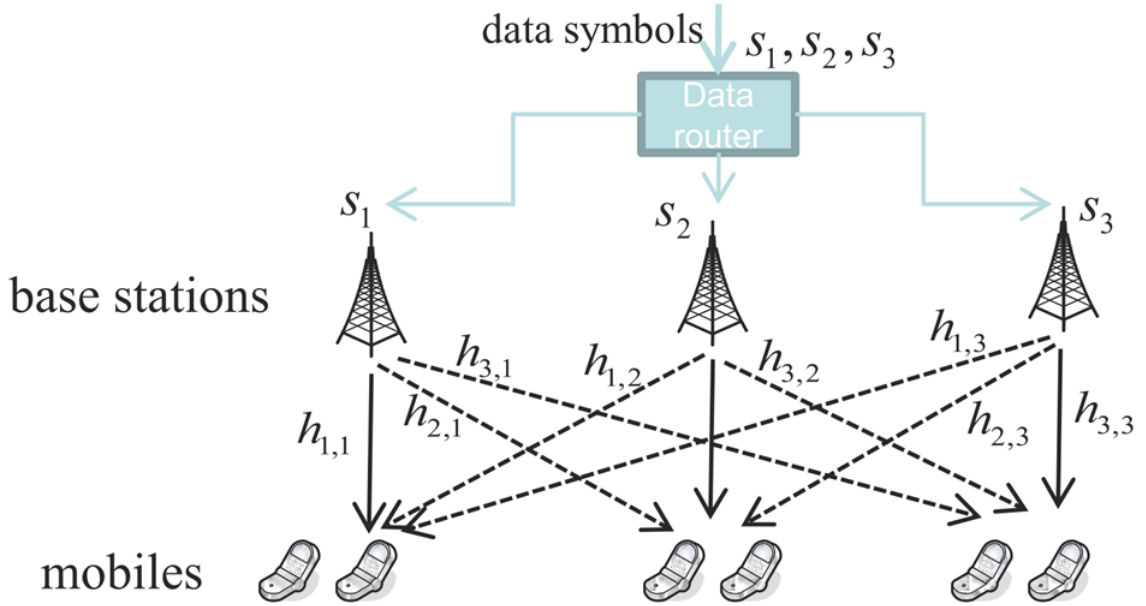


Figure 12: Principle of multi-cell processing for the downlink [19]. The data intended for a given UE is routed to all BSs and the weight used by each BS is determined based on the global CSI.

maximization of the SLNR, the transmit precoder is optimized to maximize the ratio of the power of desired signal received by a given UE to the total emitted interference power to other UEs plus the noise power. In the third design metric, which is the most popular one, the transmit precoder matrix is chosen to maximise the sum of the rates of all UEs.

3.3.3 Multi-Cell Cooperation with Limited Backhaul Capacity

In the previously discussed multi-cell processing approaches, it was assumed that there is unlimited backhaul capacity to support the sharing of global CSI and user data. However, it is quite difficult to share the user data in large networks. For this reason, several papers have proposed a multi-cell processing scheme with limited backhaul capacity. The main focus of these papers is how to form coordination areas, i.e., clusters of cells, within a large network where multi-cell processing can be applied. In addition, how to assign UEs to the clusters, and choose the optimal transmission powers and beamformers are among the considered problems. The problem of channel assignment in OFDM systems could also be considered, which makes the problem more complicated. On the other hand, cell clustering can be done statically or dynamically, where in either way it can be implemented using centralized or distributed approach.

Nevertheless, in networks with limited multi-cell cooperation, there is always inter-cluster interference. This limits the performance improvement which can be achieved, and as the signal to noise ratio (SNR) increases, the network becomes inter-cluster interference limited. To mitigate the inter-cluster interference, several approaches are proposed. One of the approaches to mitigate inter-cluster interference uses the concept of multi-shift approach, which systematically avoids the occurrence of the UEs which are being served from the cluster edge [42, 43, 44]. Another approach introduces inter-cluster negotiation to minimize the inter-cluster interference on UEs, which are found in the cluster-edge [45]. In [11], how UEs data should be routed with a constraint on the amount of data symbols, which could be routed is determined so that the emitted interference is minimized. This approach differs from other clustering approaches, since the the set of BSs which serve each UE is independently determined.

4 Sparse Precoding

In this chapter, sparse precoding is explained and applied as a multi-cell cooperation technique for minimizing inter-operator interference in chapter 5. This precoding scheme is proposed in [11] for optimized data symbol sharing with constraint on the total amount of data shared. It is applied based on sparse inverse algorithm which is an algorithm used to find an approximate inverse of a sparse matrix [48]. In addition, zero forcing criterion is used for maximizing the sum data rate. Moreover, the authors also adapted the precoding scheme for Minimizing Mean Square Error (MMSE) criterion.

4.1 Multicell Joint Transmission Channel

For the analysis in the consequent subsections, we use similar system model which consists of N single antenna BSs and M single antenna UEs. In addition, we consider only joint downlink transmission, and the received signal is given as

$$\mathbf{y} = \mathbf{H}\mathbf{x} + \boldsymbol{\eta} \quad (4)$$

$$i.e., \begin{bmatrix} y_1 \\ \vdots \\ y_M \end{bmatrix} = \begin{bmatrix} \mathbf{h}_1^H \mathbf{x} \\ \vdots \\ \mathbf{h}_M^H \mathbf{x} \end{bmatrix} + \begin{bmatrix} \eta_1 \\ \vdots \\ \eta_M \end{bmatrix}$$

where $\mathbf{y} \in \mathbb{C}^{M \times 1}$ denotes the received signal vector, $\mathbf{H} \in \mathbb{C}^{M \times N}$ denotes the complex channel gain matrix, $\mathbf{x} = [x_1, x_2, \dots, x_N]^T$ denotes the complex antenna output vector, $\mathbf{h}_m^H \in \mathbb{C}^{1 \times N}$ denotes the channel gain from all BSs to UE m , and $\boldsymbol{\eta}$ denotes the noise which is model as zero mean i.i.d. complex circularly Gaussian with variance σ^2 . In addition, y_m denotes the signal received by UE m , h_{mn} denotes the complex channel gain from BS n to UE m , x_n denotes the complex (antenna) output from BS n .

On the other hand, let us denote the vector of data symbols as $\mathbf{s} = [s_1, \dots, s_M]^T$ with s_m representing the data symbol intended for UE m . Let us also denote the precoding matrix which maps the data symbols to each antenna as $\mathbf{W} \in \mathbb{C}^{N \times M}$ with $\mathbf{w}_m \in \mathbb{C}^{N \times 1}$ representing the beamforming vector for transmitting the data symbol m . The complex antenna output is given as

$$\mathbf{x} = \mathbf{W}\mathbf{s} \quad (5)$$

This implies, the antenna output at BS n is given as

$$x_n = \sum_{m=1}^M w_{nm} s_m \quad (6)$$

In addition, the data rate achieved by the UE m is given as

$$R_m = \log_2 \left(1 + \frac{|\mathbf{h}_m^H \mathbf{w}_m|^2}{\sigma^2 + \sum_{j \neq m} |\mathbf{h}_m^H \mathbf{w}_j|^2} \right) \quad (7)$$

4.2 Optimization Criteria

4.2.1 Zero-Forcing Criterion

The aim of zero forcing criterion is to null the interference received by all UEs. In other words, if the signal vector for each UE is project away from other UEs, the received signal by each UE could be made interference-free. This can be achieved by having a precoder matrix which is simply the pseudo inverse of the complex channel matrix [34, 46]. Therefore, the precoder matrix is given as

$$\mathbf{W} = K\mathbf{H}^\dagger(\mathbf{H}\mathbf{H}^\dagger)^{-1} \quad (8)$$

where $(\cdot)^\dagger$ represents the hermitian conjugate and K is a normalisation factor based on the power constraint. For example, if we take a sum power constrain with the transmit power per each transmit antenna given as P , then K will be

$$K = \frac{NP}{\|\mathbf{H}^\dagger(\mathbf{H}\mathbf{H}^\dagger)^{-1}\|_2} \quad (9)$$

Therefore, inserting Equations 5 and 8 into Equation 4, the received signal becomes

$$\begin{aligned} \mathbf{y} &= \mathbf{H}\mathbf{x} + \eta \\ &= K\mathbf{H}\mathbf{H}^\dagger(\mathbf{H}\mathbf{H}^\dagger)^{-1} + \eta \\ &= K\mathbf{s} + \eta \end{aligned} \quad (10)$$

As shown in Equation 10, the data symbol is received without interference, while all BSs could participate in the transmission. The data rate achieved by the i^{th} UE can re-written as

$$R_i = \log_2\left(1 + \frac{|\mathbf{h}_m^H \mathbf{w}_m|^2}{\sigma^2}\right) \quad (11)$$

Several power constraints are applied to optimise a given performance metric. One of the popular power constrains is the sum power constraint with the aim of maximising the sum data rate [47]. In this case, the optimal power allocation is found using water filling. On the other hand, a per antenna power constraint could be applied for a min-max rate optimisation problem [34].

4.2.2 MMSE criterion

The MSE of Zero Forcing precoding scheme tends to zero for high Signal to Noise Ratio (SNR). However, for low SNR, optimal result cannot be achieved using zero forcing criterion. Even the rate achieved per UE tends to zero for large networks. In order to get an optimal result under all SNR values, the regularised zero forcing precoding, which sometimes is called the transmit Wiener filter, is used [46]. In this case, the precoder is given as [46, 11]

$$\mathbf{W} = K(\mathbf{H}^H\mathbf{H} + \frac{\sigma^2}{P}\mathbf{I}_N)^{-1}\mathbf{H}^H \quad (12)$$

where K a normalising constant which accounts for the applied power constraint and \mathbf{I}_N is an identity matrix of size $N \times N$.

4.3 Sparse Precoding based on Sparse Inverse Algorithm

As we have discussed in Section 3.3.3, one of the approaches to mitigate inter-cluster interference is by optimising the data routing matrix with a given constraint on the amount of data symbols which could be routed in the network [11]. In this approach, each UE is served by a subset of the BSs, minimising the emitted interference to other UEs using interference coordination. In other words, for a given routing matrix, the precoder bears the shape of the given routing matrix, and is optimised with a given performance metric such that the emitted interference to the UEs which are not served by the same subset of BSs is minimised.

First, let us consider how a routing matrix is defined before we proceed into how an optimised precoder is obtained for a given routing matrix. The entries of a routing matrix \mathbf{D} have binary values which indicate the BSs to which the data for each UE is routed. In other words, if $d_{n,m} = 1$, the data intended for UE m is routed to BS n , otherwise it is not. Accordingly, the routing matrix for the network in Fig. 13 can be expressed as

$$\begin{bmatrix} 1 & 1 & 0 \\ 1 & 1 & 0 \\ 0 & 1 & 1 \end{bmatrix}$$

As shown in Fig. 13, the data for UE 1 is routed only to BSs 1 and 2, which implies $d_{1,1} = 1$, $d_{2,1} = 1$ and $d_{3,1} = 0$. Similarly, how the data symbols for UEs 2 and 3 are routed is shown in columns 2 and 3 of the routing matrix, respectively, and obtained in a similar fashion as for column 1.

Having explained how a routing matrix is defined, let us have a brief look into how an optimised precoder which maximised the sum throughput is obtained for a given routing matrix as derived in [11]. The optimised precoder for a given routing matrix is derived based on sparse inverse algorithm [48] with zero forcing criterion. With this criterion, the maximisation of the sum throughput can be replaced by the minimisation of the emitted interference, that is,

$$\widehat{\mathbf{W}} = \arg \min_{\mathbf{W}} \|\mathbf{H}\mathbf{W} - \mathbf{I}_M\|_F^2 \quad (13)$$

where $\|\cdot\|_F$ represents the Frobenius norm.

Sum power constraint with equal per stream power is assumed; that is, $\|\mathbf{w}_m\|_2^2 = P_m = P, \forall m \in \{1, \dots, m, \dots, M\}$. With this power constraint and the aim of minimising the emitted interference, the columns of \mathbf{W} can be computed independently. This implies, for a given routing matrix \mathbf{D} , the beamforming vector \mathbf{w}_m for transmitting symbol m , i.e., the data symbol intended for UE m , can be computed from the following minimization problem

$$\hat{\mathbf{w}}_m = \arg \min_{\tilde{\mathbf{w}}_m} \|\mathbf{H}\tilde{\mathbf{w}}_m - \mathbf{e}_m\|_2^2 \quad (14)$$

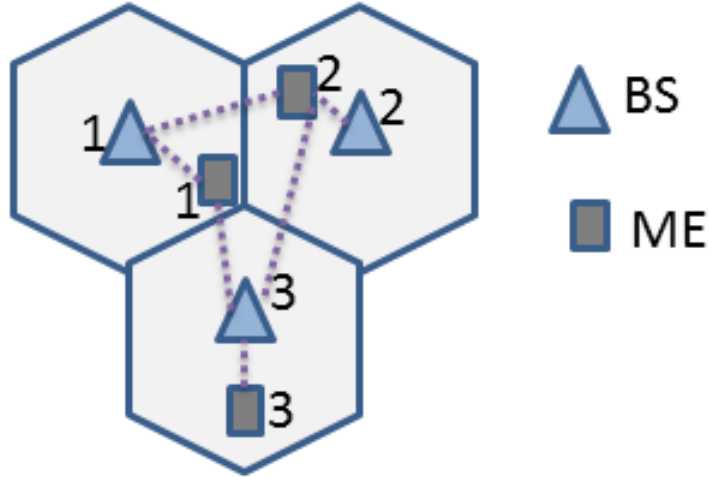


Figure 13: A simple network with a simple data routing where the data symbol for UE 1 is routed to BSs 1 and 2, for UE 2 is routed to BSs 1,2 and 3, and for UE 3 is routed to BS 3.

where the vector \mathbf{e}_m is the column m of the identity matrix and the beamforming vector $\tilde{\mathbf{w}}_m$ is the column m of the precoding matrix but bearing the shape of \mathbf{d}_m , i.e., $\tilde{\mathbf{w}}_m = \mathbf{d}_m \odot \mathbf{w}_m$, where \mathbf{d}_m is the column m of \mathbf{D} and \odot represents the element wise multiplication.

Since the minimisation problem in Equation 14 is a least squares problem¹, it can be solved using QR decomposition approach. In addition, if the routing matrix \mathbf{D} is a parse matrix, the computation can be simplified by systematically avoiding the entries which lead to identically zero column or row vectors in the calculation. For this purpose, let us denote the set of indices j such that $\tilde{\mathbf{w}}_m(j) \neq 0$ by \mathcal{J} , and the set of indices m such that $\mathbf{H}(m, \mathcal{J})$ is not identically zero, i.e., by \mathcal{I} . In addition, let $|\mathcal{J}| = \eta_2$ and $|\mathcal{I}| = \eta_1$, where in this case $|\cdot|$ represents the cardinality. Moreover, let us denote the reduced channel matrix $\mathbf{H}(\mathcal{I}, \mathcal{J}) \in \mathbb{C}^{\eta_1 \times \eta_2}$ by $\tilde{\mathbf{H}}$, and the reduce canonical vector $\mathbf{e}_m(\mathcal{J})$ by $\tilde{\mathbf{e}}_m$. The objective of the least squares problem in Equation 14 can be re-written as

$$\hat{\mathbf{w}}_m = \arg \min_{\tilde{\mathbf{w}}_m} \|\tilde{\mathbf{H}}\tilde{\mathbf{w}}_m - \tilde{\mathbf{e}}_m\|_2^2 \quad (15)$$

The solution to Equation 15 is readily found using the QR-decomposition method. Let the QR decomposition of $\tilde{\mathbf{H}}$ be given as

$$\tilde{\mathbf{H}} = \tilde{\mathbf{Q}} \begin{bmatrix} \tilde{\mathbf{R}} \\ \mathbf{0}_{(\eta_1 - \eta_2) \times \eta_2} \end{bmatrix} \quad (16)$$

where $\tilde{\mathbf{Q}} \in \mathbb{C}^{\eta_1 \times \eta_1}$ is an orthonormal matrix, $\tilde{\mathbf{R}} \in \mathbb{C}^{\eta_2 \times \eta_2}$ is an upper triangular

¹Least squares problem is discussed in Appendix A.

matrix and $\mathbf{0}_{(\eta_1-\eta_2)\times\eta_2}$ is a zero matrix of size $(\eta_1 - \eta_2) \times \eta_2$.

The solution can then be expressed as

$$\tilde{\mathbf{w}}_m = K \begin{bmatrix} \tilde{\mathbf{R}}^{-1} & \mathbf{0}_{\eta_2 \times (\eta_1 - \eta_2)} \end{bmatrix} \tilde{\mathbf{Q}}^H \tilde{\mathbf{e}}_m \quad (17)$$

The normalizing constant K accounts for the applied power constraint, and with the equal per stream power constraint that we considered, Equation 42 becomes

$$\tilde{\mathbf{w}}_m = \sqrt{P} \frac{\begin{bmatrix} \tilde{\mathbf{R}}^{-1} & \mathbf{0}_{\eta_2 \times (\eta_1 - \eta_2)} \end{bmatrix} \tilde{\mathbf{Q}}^H \tilde{\mathbf{e}}_m}{\left\| \begin{bmatrix} \tilde{\mathbf{R}}^{-1} & \mathbf{0}_{\eta_2 \times (\eta_1 - \eta_2)} \end{bmatrix} \tilde{\mathbf{Q}}^H \tilde{\mathbf{e}}_m \right\|} \quad (18)$$

Sparse precoding with zero forcing criterion has been explained. Interested readers can find the adaptation of sparse precoding for MMSE criterion in [11].

5 Dynamic Spectrum Sharing between Co-located RANs

In this Chapter, we propose a heuristic algorithm based on user grouping for efficient spectrum sharing among co-located RANs. Each RAN is assumed to be owned by separate operators. The main aim of the algorithm is to dynamically partition the available spectrum into private and shared frequency sub-bands, see Fig. 14. The private frequency sub-bands are independently used by each RAN, while the shared frequency sub-band is shared among the RANs non-orthogonally. The available spectrum can be assumed to be a new available spectrum for joint use by the operators, or the sum of all the licensed spectrum to the operators.

Specifically, we consider only the co-existence of two RANs, as shown in Fig. 15. The two RANs are assumed to be connected using fiber optics merely for the purpose of exchanging CSI and control information. Due to the requirement for extremely high capacity and low latency backhaul, it is assumed that data sharing between the RANs is impractical. However, within each RAN, we assume that the user data is fully shared. We further assume, either the two RANs implement the proposed algorithm independently using similar global CSI to reach at the same result, or the two RANs only exchange inter-RAN CSI, sum rates achieved by the UEs served in the private frequency sub-band and other necessary signalling information necessary to implement the proposed algorithm.

From the assumptions taken on the intra-and inter-RAN backhaul capacity, applying multi-cell cooperation for managing interference will be suitable. Multi-cell processing technique is applied for jointly serving the UEs scheduled in the private frequency sub-band of each RAN, while interference coordination technique is used for minimising the inter-RAN interference when serving UEs on the shared frequency sub-band. Particularly, Zero forcing precoder is used to jointly serve the UEs scheduled in the private frequency sub-bands. For those UEs scheduled in the shared frequency sub-band, Sparse precoding, which was discussed in Chapter 4, is applied minimising inter-operator interference. The data routing matrix of the UEs served in the shared frequency sub-band is typically sparse due to the restriction

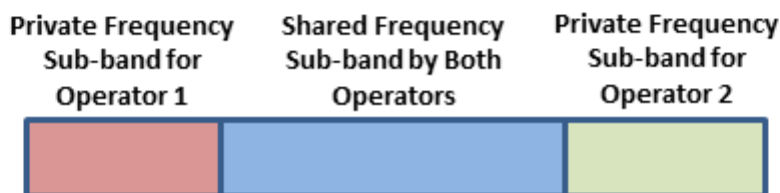


Figure 14: Illustration of Dynamic Spectrum Allocation. The total available spectrum is partitioned into private and shared (in a non-orthogonal way) frequency sub-bands in an adaptive way.

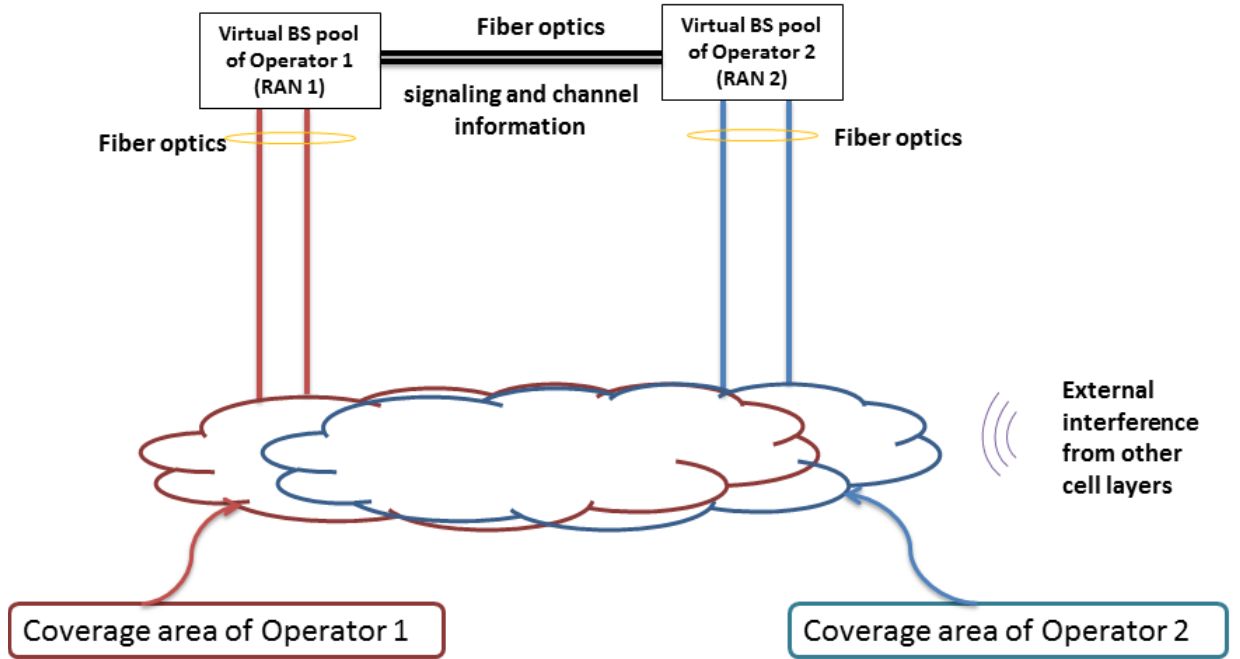


Figure 15: An illustration of co-located RANs. The BSs/RRHs of each RAN are assumed to be connected to a virtual BS pool using fiber optics. Further, the two virtual BS pool are assumed to be connected using fiber optics for the exchange of CSI and signalling information

that data symbols cannot be shared between the RANs and the number of UEs served in the shared frequency sub-band is typically less than the total number of UEs. This makes it suitable to apply Sparse precoding scheme. Both the intra- and inter-precoders are assumed to use equal per stream power constraint, which implicitly indicates that sum power constraint needs to be fulfilled as well. As it will be shown in later sections, the described intra- and inter-RAN precoders are taken into consideration when optimizing the partitioning of the spectrum into private and shared frequency sub-bands.

In the subsequent sections, the system model is first explained. Next, the optimization problem is formulated. Finally, the proposed heuristic algorithm based on user grouping is explained.

5.1 System Model

5.1.1 Multi-RAN Joint Transmission Channel

We consider a downlink multi-RAN joint transmission system consisting of two RANs. The first RAN is owned by operator 1 and consists of M_1 BSs which jointly serve M_1 UEs. The second RAN is owned by operator 2 and consists of M_2 BSs which

jointly serve M_2 UEs. Let us denote the total available spectrum for both operators as B , out of which B_s is shared by both operators in a non-orthogonal way, B_{p_1} is privately used by operator 1 and B_{p_2} by operator 2. We assume $B_{p_1} = B_{p_2} = B_p$ since each operator do not want to share more bandwidth than the other.

The RANs serve the UEs scheduled in the private frequency sub-band using zero forcing precoder. On the other hand, Sparse precoder is used as inter-RANs precoder to serve the UEs scheduled in the shared frequency sub-band minimizing inter-operator interference. Let us denote the set of UEs scheduled in the private frequency sub-band as $\mathcal{U}^{(p)}$ and those scheduled in the shared frequency sub-band as $\mathcal{U}^{(s)}$ where $\mathcal{U}^{(p)} \cup \mathcal{U}^{(s)} = \{1, \dots, M_1, M_1 + 1, \dots, M\}$ and $\mathcal{U}^{(p)} \cap \mathcal{U}^{(s)} = \phi$. Let us additionally represent the set of UEs scheduled in the private frequency sub-band for the first RAN as $\mathcal{U}^{(p_1)}$ where $\mathcal{U}^{(p_1)} = \mathcal{U}^{(p)} \cap \mathcal{O}^{(1)}$ and $\mathcal{O}^{(1)} = \{1, \dots, M_1\}$, while of those UEs scheduled in the frequency sub-band for the second RAN as $\mathcal{U}^{(p_2)}$ where $\mathcal{U}^{(p_2)} = \mathcal{U}^{(p)} \cap \mathcal{O}^{(2)}$ and $\mathcal{O}^{(2)} = \{M_1 + 1, \dots, M\}$. Note that a given UE is scheduled either in the private or shared frequency sub-band during one scheduling interval. The channel is modelled by the distance dependent path loss and the fast fading component. The fast fading component is assumed to follow a flat Rayleigh distribution. The noise is modelled as zero mean i.i.d complex circularly symmetric Gaussian distributed with variance σ^2 , i.e. $\mathcal{CN}(0, \sigma^2)$. Moreover, the background interference is included in the received signal so that inter-tire interference will be modelled if exists.

Before expressing the received signal mathematically, we introduce a notation² $s_i^{\mathcal{A}}$ to mean the i^{th} smallest element of a set $\mathcal{A} \subset \{1, 2, 3, \dots\}$. Now, the received signal by the UEs scheduled in the private frequency sub-band of RAN $r \in \{1, 2\}$ can be expressed as

$$\mathbf{y}^{(p_r)} = \mathbf{H}^{(p_r)} \mathbf{W}^{(p_r)} \mathbf{s}^{(p_r)} + \boldsymbol{\lambda}^{(p_r)} + \boldsymbol{\eta}^{(p_r)} \quad (19)$$

where the vectors $\mathbf{y}^{(p_r)}, \boldsymbol{\lambda}^{(p_r)}, \boldsymbol{\eta}^{(p_r)} \in \mathbb{C}^{|\mathcal{U}^{(p_r)}| \times 1}$ respectively denote the received signal, background interference, and noise vector of the UEs scheduled in the private frequency sub-band of RAN r , with $\mathbf{y}_i^{(p_r)}, \boldsymbol{\lambda}_i^{(p_r)}, \boldsymbol{\eta}_i^{(p_r)}$ respectively being the received signal, background interference, and noise by UE $s_i^{\mathcal{U}^{(p_r)}}$. The matrix $\mathbf{H}^{(p_r)} \in \mathbb{C}^{|\mathcal{U}^{(p_r)}| \times |\mathcal{O}^{(r)}|}$

²NOTATIONS:

1. $s_i^{\mathcal{A}}$ to mean the i^{th} smallest element of a set $\mathcal{A} \subset \{1, 2, 3, \dots\}$, $i \in \{1, 2, \dots\}$.
2. The indexes $(\cdot)_{(i, \cdot)}$ and $(\cdot)_{(\cdot, j)}$ respectively means the i^{th} row and j^{th} column of a matrix.
3. The symbol \odot means an element wise multiplication between two matrices.
4. The cardinality of a set \mathcal{A} is represented by $|\mathcal{A}|$.
5. The symbols $(\cdot)^\dagger$ and $(\cdot)^{-1}$ represent the Hermitian conjugate and inverse of a matrix, respectively.
6. A norm of a vector is denoted by $\|(\cdot)\|_2$.
7. A Frobenius norm of a matrix is written as $\|(\cdot)\|_F$.

denotes the r^{th} RAN's intra-operator global CSI where $\mathbf{H}_{(i,j)}^{(p_r)}$ is the complex channel gain from BS $s_j^{\mathcal{O}^r}$ to UE $s_i^{\mathcal{U}^{(p_r)}} \in \mathcal{U}^{(p_r)}$. The vector $\mathbf{s}^{(p_r)} \in \mathbb{C}^{|\mathcal{U}^{(p_r)}| \times 1}$ denotes the data symbol for the UEs scheduled in the private frequency sub-band of RAN r with $\mathbf{s}_i^{(p_r)} \in \mathcal{CN}(0, 1)$ being the data symbols for UE $s_i^{\mathcal{U}^{(p_r)}}$. The intra-RAN precoder matrix of RAN r is represented by $\mathbf{W}^{(p_r)} \in \mathbb{C}^{|\mathcal{O}^{(r)}| \times |\mathcal{U}^{(p_r)}|}$ where $\mathbf{W}_{(\cdot,j)}^{(p_r)}$ is the beamforming vector for transmitting data symbol for UE $s_j^{\mathcal{U}^{(p_r)}} \in \mathcal{U}^{(p_r)}$. The index $(\cdot)_{(\cdot,j)}$ means the j^{th} column of a matrix.

Since the intra-RAN precoders use zero forcing precoder with equal per stream power constraint, i.e. $\|\mathbf{W}_{(\cdot,j)}^{(p_r)}\|_2^2 = P$, the beamforming vector applied for transmitting the data symbol $s_j^{\mathcal{U}^{(p_r)}} \in \mathcal{U}^{(p_r)}$ can be expressed as

$$\mathbf{W}_{(\cdot,j)}^{(p_r)} = \sqrt{P} \frac{((\mathbf{H}^{(p_r)})^\dagger (\mathbf{H}^{(p_r)} (\mathbf{H}^{(p_r)})^\dagger)^{-1})_{(\cdot,j)}}{\|((\mathbf{H}^{(p_r)})^\dagger (\mathbf{H}^{(p_r)} (\mathbf{H}^{(p_r)})^\dagger)^{-1})_{(\cdot,j)}\|_2} \quad (20)$$

where $(\cdot)^\dagger$ and $(\cdot)^{-1}$ representing the Hermitian conjugate and inverse of a matrix, respectively.

On the other hand, the received signal by the UEs served in the shared frequency sub-band can be expressed as

$$\mathbf{y}^{(s)} = \mathbf{H}^{(s)} \mathbf{W}^{(s)} \mathbf{s}^{(s)} + \boldsymbol{\lambda}^{(s)} + \boldsymbol{\eta}^{(s)} \quad (21)$$

where the vectors $\mathbf{y}^{(s)}, \boldsymbol{\lambda}^{(s)}, \boldsymbol{\eta}^{(s)} \in \mathbb{C}^{|\mathcal{U}^{(s)}| \times 1}$ respectively denote the received signal, background interference, and noise of the UEs scheduled in the shared frequency sub-band, with $\mathbf{y}_i^{(s)}, \boldsymbol{\lambda}_i^{(s)}, \boldsymbol{\eta}_i^{(s)}$ respectively being the received signal, background interference, and noise by UE $s_i^{\mathcal{U}^{(s)}}$. The matrix $\mathbf{H}^{(s)} \in \mathbb{C}^{|\mathcal{U}^{(s)}| \times M}$ denotes the inter-RAN global CSI where $\mathbf{H}_{(i,j)}^{(s)}$ is the complex channel gain from BS j to UE $s_i^{\mathcal{U}^{(s)}} \in \mathcal{U}^{(s)}$. The vector $\mathbf{s}^{(s)} \in \mathbb{C}^{|\mathcal{U}^{(s)}| \times 1}$ denotes the data symbol for the UEs scheduled in the shared frequency sub-band with $\mathbf{s}_i^{(s)}$ being the data symbols for UE $s_i^{\mathcal{U}^{(s)}} \in \mathcal{U}^{(s)}$. The inter-RAN precoder matrix is represented by $\mathbf{W}^{(s)} \in \mathbb{C}^{M \times |\mathcal{U}^{(s)}|}$ where $\mathbf{W}_{(\cdot,j)}^{(s)}$ is the beamforming vector for transmitting data symbol $s_j^{\mathcal{U}^{(s)}} \in \mathcal{U}^{(s)}$.

Sparse precoder is used as inter-RAN precoder minimizing inter-RAN interference. Due to the restriction that data symbols cannot be shared among the RANs, the inter-RAN precoder $\mathbf{W}^{(s)}$ is sparse where half of its entries are zeros. The routing matrix $\mathbf{D}^{(s)} \in \{0, 1\}^{M \times |\mathcal{U}^{(s)}|}$ for $\mathbf{W}^{(s)}$ can be defined as follows

$$\mathbf{D}_{(i,j)}^{(s)} = \begin{cases} 1 & \text{if } s_i^{\mathcal{U}^{(s)}} \in \mathcal{O}^{(k)}, s_j^{\mathcal{U}^{(s)}} \in \mathcal{O}^{(l)}, k = l \\ 0 & \text{otherwise} \end{cases} \quad (22)$$

Therefore, with the defined routing matrix $\mathbf{D}^{(s)}$ and the given inter-RAN global CSI $\mathbf{H}^{(s)}$, the inter-RAN precoder matrix $\mathbf{W}^{(s)}$ is found according to the procedure in Section 4.3.

Alternative Representation of Received Signal Vector

Alternatively³, the received signal can be expressed with a single compact equation which gives more insight into how the Sparse precoder works. Let us denote the complex channel gain matrix from all the BSs of both RANs to all their UEs as $\mathbf{H} \in \mathbb{C}^{M \times M}$, where $\mathbf{H}_{(i,j)}$ denotes the complex channel gain from BS j to UE i . Let us represent the intra-and inter-RAN precoders by $\mathbf{W} \in \mathbb{C}^{M \times M}$ and $\widetilde{\mathbf{W}} \in \mathbb{C}^{M \times M}$, respectively. The beamforming weight $\mathbf{W}_{(i,j)}$ is non-zero if the data symbol for UE j scheduled in the private frequency sub-band is shared with BS i . Similarly, The beamforming weight $\widetilde{\mathbf{W}}_{(i,j)}$ is non-zero if the data symbol for UE j scheduled in the shared frequency sub-band is shared with BS i .

The alternative representation of the received signal can be written as

$$\mathbf{y} = (\mathbf{H} \odot \mathbf{F})\mathbf{W}\mathbf{s} + (\mathbf{H} \odot \widetilde{\mathbf{F}})\widetilde{\mathbf{W}}\mathbf{s} + \boldsymbol{\lambda} + \boldsymbol{\eta} \quad (23)$$

where the symbol \odot denotes element-wise multiplication of two matrices. The vector $\mathbf{y} \in \mathbb{C}^{M \times 1}$ represents the received signal vector with y_i being the received signal by UE i . The matrices $\mathbf{F}, \widetilde{\mathbf{F}} \in \{0, 1\}^{M \times M}$ are introduced to nullify the unnecessary entries of the matrix \mathbf{H} when computing the precoder matrices for serving the UEs scheduled in the private and shared frequency sub-bands, respectively. The vectors $\mathbf{s}, \boldsymbol{\lambda}, \boldsymbol{\eta} \in \mathbb{C}^{M \times 1}$ denote the data symbols, the external interference and the noise vectors, respectively where $s_i \in \mathcal{CN}(0, 1)$ is the data symbol for UE i , and λ_i and η_i are the received interference and noise signal by UE i , respectively.

For a given user scheduling decision $\mathcal{U} = \{\mathcal{U}^{(p)}, \mathcal{U}^{(s)}\}$, the matrices \mathbf{F} and $\widetilde{\mathbf{F}}$ are defined as

$$\mathbf{F}_{(i,j)} = \begin{cases} 1 & \text{if } i \in \mathcal{U}^{(p)}, i \in \mathcal{O}^{(k)}, j \in \mathcal{O}^{(l)}, k = l \\ 0 & \text{otherwise} \end{cases} \quad (24)$$

$$\widetilde{\mathbf{F}}_{(i,j)} = \begin{cases} 1 & \text{if } i \in \mathcal{U}^{(s)} \\ 0 & \text{otherwise} \end{cases} \quad (25)$$

In addition, if we denote the routing matrices for the precoder matrices \mathbf{W} and $\widetilde{\mathbf{W}}$ as \mathbf{D} and $\widetilde{\mathbf{D}}$, respectively, they can be defined as

$$\mathbf{D}_{(i,j)} = \begin{cases} 1 & \text{if } i \in \mathcal{U}^{(p)}, i \in \mathcal{O}^{(k)}, j \in \mathcal{O}^{(l)}, k = l \\ 0 & \text{otherwise} \end{cases} \quad (26)$$

$$\widetilde{\mathbf{D}}_{(i,j)} = \begin{cases} 1 & \text{if } i \in \mathcal{U}^{(s)}, i \in \mathcal{O}^{(k)}, j \in \mathcal{O}^{(l)}, k = l \\ 0 & \text{otherwise} \end{cases} \quad (27)$$

We, therefore, have $\mathbf{W} = \mathbf{W} \odot \mathbf{D}$ and $\widetilde{\mathbf{W}} = \widetilde{\mathbf{W}} \odot \widetilde{\mathbf{D}}$.

³This alternative representation is solely added for the purpose illustrating how the Sparse precoder works and could generalize matrix pseudo-inversion.

The precoder matrix \mathbf{W} is sparse and it contains all the entries of the precoder matrices $\mathbf{W}^{(p_r)}$, $r \in \{1, 2\}$. The beamforming vector of a UE $i \in \mathcal{U}^{(p_r)}$ is solely determined using the intra-RAN CSI, i.e. $\mathbf{H}^{(p_r)}$. Consider the computation of the beamforming vector $\mathbf{W}_{(\cdot,j)}$ of a UE $j \in \mathcal{U}^{(p_r)}$ using the procedure for sparse precoding. According to the precoder matrix, the set of the non-zero entries of the beamforming vector is $\mathcal{I} = \{i \mid \mathbf{D}_{(i,j)} = 0\}$. Due to the definition of \mathbf{B} , $\mathcal{I} = \mathcal{O}^{(r)}$. In addition, the set of identically zero rows of $(\mathbf{H} \odot \mathbf{F})_{(\mathcal{I},\cdot)}$ is $\mathcal{J} = \{k \mid (\mathbf{H} \odot \mathbf{F})_{(\mathcal{I},k)} = 0\}$. Therefore, the reduced channel matrix is equal to the intra-RAN CSI, that is $(\mathbf{H} \odot \mathbf{F})_{(\mathcal{I},\mathcal{J})} = \mathbf{H}^{(p_r)}$, and the beamforming vector is found as follows:

$$\mathbf{W}_{(\mathcal{I},j)}^* = \min_{\mathbf{w}_{(\mathcal{I},j)}} \|\mathbf{H}^{(p_r)} \mathbf{w}_{(\mathcal{I},j)} - \mathbf{e}_j\|_2^2 \quad (28)$$

where $\mathbf{e}_j \in \{0, 1\}^{|\mathcal{I}| \times 1}$, having its j -th element a non-zero value and the rest of its elements a value of zero. The minimization problem is a least squares problem⁴, and one possible way to solve the problem is using QR-decomposition according.

Since the precoder matrices $\mathbf{W}^{(p_r)}$, $r \in \{1, 2\}$ are found by minimizing the Frobenius norm $\|\mathbf{H}^{(p_r)} \mathbf{W}^{(p_r)} - \mathbf{I}_{M_r}\|_F$, $\mathcal{I} = \mathcal{O}^{(r)}$ and we have [48]

$$\|\mathbf{H}^{(p_r)} \mathbf{W}^{(p_r)} - \mathbf{I}_{M_r}\|_F^2 = \sum_{j \in \mathcal{U}^{(p_r)}} \|\mathbf{H}^{(p_r)} \mathbf{w}_{(\cdot,j)}^{(p_r)} - \mathbf{e}_j\|_2^2, \quad (29)$$

we are computing the j -th column of $\mathbf{W}^{(p_r)}$ by Equation 39, i.e. $\mathbf{W}_{(\mathcal{I},j)}^* = \mathbf{W}^{(p_r)}$. Therefore, the matrices $\mathbf{W}^{(p_r)}$, $r \in 1, 2$ are computed independently using their own intra-RAN CSI when computing the precoder \mathbf{W} using sparse precoding. Similar analysis could be used to reach at the conclusion that the entries of the precoder matrix $\mathbf{W}^{(s)}$, which is used to serve the users in the shared frequency sub-band, are also computed when computing $\widetilde{\mathbf{W}}$ using sparse precoding.

5.1.2 System Performance Model

The data rate of a UE is used for measuring its performance. The data rate of a UE depends on the operational bandwidth and the received SINR. Therefore, a UE $k = s_i^{\mathcal{U}^{(p_r)}}$ which is served in the private frequency sub-band of RAN r achieves a data rate of

$$R_k^{(p_r)} = B_p \log_2 \left(1 + \frac{|\mathbf{H}_{(i,\cdot)}^{(p_r)} \mathbf{w}_{(\cdot,i)}^{(p_r)}|^2}{\sigma^2 + \lambda_i + \sum_{j \neq i} |\mathbf{H}_{(i,\cdot)}^{(p_r)} \mathbf{w}_{(\cdot,j)}^{(p_r)}|^2} \right) \quad (30)$$

and a UE $k = s_i^{\mathcal{U}^{(s)}}$ which is served in the shared frequency sub-band achieves a data rate of

$$R_k^{(s)} = B_s \log_2 \left(1 + \frac{|\mathbf{H}_{(i,\cdot)}^{(s)} \mathbf{w}_{(\cdot,i)}^{(s)}|^2}{\sigma^2 + \lambda_i + \sum_{j \neq i} |\mathbf{H}_{(i,\cdot)}^{(s)} \mathbf{w}_{(\cdot,j)}^{(s)}|^2} \right) \quad (31)$$

⁴Least squares problem is discussed in Appendix A.

Note that the sum term in the denominator of Equation 30 is zero since $\mathbf{W}^{(p_r)}$ is a zero forcing precoder and the data symbols are shared among all the BSs of RAN r . However, the sum term in the denominator of Equation 31 is not zero as the data symbols for the UEs scheduled in the shared frequency sub-band are not shared among the BS of different RANs and thus the inter-RAN interference cannot be forced to zero. The effect of the inter-RAN on the rate depends on its strength when compared to the external interference plus noise power.

5.2 Dynamic Spectrum Sharing

5.2.1 Optimisation Problem

The maximisation of the inter-RAN sum rate, i.e the sum of the data rates of all the UEs of both RANs, is considered by partitioning the spectrum into private and shared parts, and grouping the UEs to be served into either part. Let us use a set $\mathcal{U} = \{\mathcal{U}^{(p)}, \mathcal{U}^{(s)}\}$ to denote all the possible scheduling decisions to schedule part of the UEs in the private frequency sub-band and the other part in the shared frequency sub-band, and a set $\mathcal{B} = \{B_p, B_s\}$ to represent all the possible ways of partition the total available spectrum into private and shared frequency sub-bands. The optimization problem can be mathematically expressed as

$$\begin{aligned}
& \underset{\mathcal{U}, \mathcal{B}}{\text{maximize}} && \sum_{r=1}^2 \sum_{i \in \mathcal{U}^{(p_r)}} R_i^{(p_r)} + \sum_{j \in \mathcal{U}^{(s)}} R_j^{(s)} \\
& \text{subject to} && \mathcal{U}^{(p)} \cup \mathcal{U}^{(s)} = \{1, \dots, M\} \\
& && \mathcal{U}^{(p)} \cap \mathcal{U}^{(s)} = \phi \\
& && 2B_p + B_s = B \\
& && \|\mathbf{W}_{(\cdot, j)}^{(p_r)}\|_2^2 = P, \forall j \in \mathcal{U}^{(p_r)}, r \in 0, 1 \\
& && \|\mathbf{W}_{(\cdot, j)}^{(s)}\|_2^2 = P, \forall j \in \mathcal{U}^{(s)}
\end{aligned} \tag{32}$$

The double sum in the objective function is the sum of the rates of the UEs scheduled in the private frequency sub-band, while the last sum term is the sum of the rates of the UEs scheduled in the shared frequency sub-band. The first two constraints account for the restriction that a given UE could be scheduled either in the private or shared frequency sub-band at a time. The third constraint is due to the fact that the total available spectrum for both RANs is B Hz. The last two constraints indicates that equal per stream power constraint is applied. They also implicitly indicate that the sum power constraint is fulfilled.

In the optimization problem, the individual and inter-RAN sum rate generally depend on

1. *How the spectrum is partitioned into private and shared frequency sub-bands;*
2. *How the UEs are grouped to be served in the private and shared frequency sub-bands;*

3. The precoding matrices.

From the perspective of a given UE, its data rate depends on its received SINR and its operational bandwidth. The higher the number of UEs which are scheduled with the UE, the lower the spectral efficiency the UE achieves since joint transmission is used. In addition, the higher the amount of operational bandwidth given to the UE, the higher the rate the UE achieves. The amount of the operational bandwidth might affect the SINR that a UE gets depending on the strength of the external interference plus noise which depend on the operational bandwidth.

5.2.2 Heuristic Algorithm based on User Grouping

We use a heuristic search to find a sub-optimal solution. However, the rate achieved using the algorithm is guaranteed to be higher than or equal to the rate which could be achieved by the conventional approaches of orthogonal, i.e. $\mathcal{B} = \{B/2, 0\}$, and full, i.e. $\mathcal{B} = \{0, B\}$, spectrum allocations. In the algorithm, the scheduling of the UEs into the orthogonal and shared frequency sub-bands (user grouping) for a given spectrum allocation is done based on an ad-hoc measure. The optimization over the spectrum allocations is done first by limiting the set of spectrum allocations into a fixed number, which depends on the computational capacity of the scheduler, and then searching exhaustively for the spectrum allocation leading to the maximum inter-RAN sum rate among the limited set of spectrum allocations. Since in the limited set of spectrum allocations, the orthogonal spectrum allocation and full spectrum allocations are always included, we are guaranteed that the achieved inter-RAN sum rate is higher than the rate which could be achieved using orthogonal and full spectrum allocations both on short and long time scales.

The algorithm could be implemented by exchanging inter-RAN global CSI, beamforming vectors for serving the UEs in the shared frequency sub-band and the achieved (sum) rates of the UEs served by each RAN. The intra-RAN precoder is computed using intra-RAN global CSI independently by each RAN. Due to the equal per stream power constraint, the beamforming vector for serving the UEs scheduled in the shared frequency sub-band is independently computed. Thus, each RAN could be assumed to compute the beamforming for serving its UEs scheduled in the shared frequency sub-band independent of the other RAN except for the inter-RAN global CSI.

A. User grouping for a fixed spectrum allocation

For a given spectrum partition $\mathcal{B} = \{B_p, B_s\}$, the problem of optimizing the user grouping, i.e. $\mathcal{U} = \{\mathcal{U}^{(p)}, \mathcal{U}^{(s)}\}$, to maximize the inter-RAN sum rate is a combinatorial problem. One approach to maximize the inter-RAN sum rate is by maximizing the individual rate of the UEs, i.e. by scheduling each UE on the frequency sub-band where it could achieve a better rate. The rate of a UE depends on the combined effect of the operational bandwidth and the achieved spectral efficiency. The operational bandwidth of the UEs which would be scheduled in either the private or

shared frequency sub-band is given. However, the spectral efficiency that a given UE could achieve depends on the number, position and CSI of the UEs jointly served with the UE in the same frequency sub-band, where the group of UEs to be scheduled in the same frequency sub-band is yet to be optimized.

There could be several ways to optimize the user grouping for a given spectrum partition. An exhaustive search might be used to find the optimal user grouping, however it is in-feasible for our purpose due to its high computational demand as the size of the set \mathcal{U} is quite high for high number of UEs. Another approach might be to use a greedy search where starting from the user group $\mathcal{U} = \{\{1, \dots, M\}, \phi\}$, the set \mathcal{U} is updated by iteratively checking if a UE tentatively scheduled in the private frequency sub-band would rather prefer to be scheduled on the shared frequency sub-band (where the updated \mathcal{U} in the previous iteration is taken in to account when estimating rates for the UE). However, since the optimization of user grouping is done over a set of spectrum partitions, the use of greedy search would also be computational demanding.

To reduce the computational demand, a simple ad-hoc measure is used where an estimated spectral efficiency that a UE would achieve based on a worst case scenario is used in order to decide in which frequency sub-band to schedule the UE. A UE scheduled in the frequency sub-band achieves the lowest spectral efficiency if all the UEs belonging to its serving RAN are served in the private frequency sub-band. Similarly, a UE scheduled in the shared frequency sub-band achieves the lowest spectral efficiency if all the UEs belonging to both RANs are scheduled in the shared frequency sub-band. Let us denote the spectral efficiencies that a UE $i \in \{1, \dots, M\}$ could achieve if it is scheduled with all the UEs in the private and shared frequency sub-bands by $S_i(\{\{1, \dots, M\}, \phi\})$ and $S_i(\{\phi, \{1, \dots, M\}\})$, respectively. A given UE is then scheduled in the private frequency sub-band if $B_p \times S_i(\{\{1, \dots, M\}, \phi\}) \geq B_s \times S_i(\{\phi, \{1, \dots, M\}\})$. Otherwise, it is scheduled in the shared frequency sub-band.

The advantage of such an approach is that the spectral efficiencies $S_i(\{\{1, \dots, M\}, \phi\})$ and $S_i(\{\phi, \{1, \dots, M\}\})$ are independent of the spectrum partition and they need to be computed only once when optimizing over the set of spectrum partitions. The approach is, therefore, less computationally demanding, however, at the cost of the efficiency of the solution. Note that, however, the $S_i(\{\{1, \dots, M\}, \phi\})$ and $S_i(\{\phi, \{1, \dots, M\}\})$ are solely used for determining the user grouping for a given spectrum partition. The real spectral efficiency that a UE would achieve after the user grouping (for a given spectral efficiency) and thus the real rate of the UE are used when searching for the maximum inter-RAN sum rate over the set of spectrum partitions.

B. Optimization over the set of spectrum partitions

The inter-RAN sum rate is optimized over the set of spectrum partitions by limiting the size of the set into computationally tractable size, and exhaustively searching for the maximum inter-RAN sum rate over the limited set. If the available spectrum is assumed to be infinitely divisible, we could have infinite ways of dividing the spectrum into private and shared frequency sub-bands. In systems employing OFDMA, the spectrum could flexibly allocated in as small amount as a resource block. Therefore, the set of spectrum allocations is generally too large and computationally demanding to exhaustively search for the optimal spectrum partition.

We introduce a parameter K to limit the set of spectrum partitions taking into consideration the computational capacity of the RANs. With the parameter K , the set of the limited spectrum partitions is defined as:

$$\mathcal{B}^{(\text{limited})} = \{0.5B(K - k)/K, Bk/K \mid k \in \{0, 1, \dots, K\}, K \in \{1, 2, \dots\}\} \quad (33)$$

For a given spectral partition, the set \mathcal{U} is determined as in Subsection 5.2.2A. The intra-and inter-RAN precoders are then computed as in Section 5.1. The data rates of the UEs scheduled in the private and shared frequency sub-bands are then calculated as in Subsection 5.1.2. The inter-RAN sum rate is finally computed which corresponds to the given spectrum partition. The maximum inter-RAN sum rate is searched over the limited set of the spectrum partitions as summarized in Algorithm 1.

Algorithm 1 Heuristic Algorithm based on User Grouping

```

GIVEN:  $K \in \{1, 2, \dots\}$ 
DENOTE: Inter-RAN sum rate by  $R$ 
INITIALIZE:  $R^* = 0$ ,  $\mathcal{B}^* = \{0.5B, 0\}$ ,  $\mathcal{U}^* = \{\{1, \dots, M\}, \phi\}$ 
for  $k \in \{0, 1, \dots, K\}$  do
  INITIALIZE:  $\mathcal{U}^{(p)} = \phi$ ,  $\mathcal{U}^{(s)} = \phi$ 
   $\mathcal{B} = \{0.5B(K - k)/K, Bk/K\} \implies B_p = 0.5B(K - k)/K, B_s = Bk/K$ 
  for  $m \in \{0, 1, \dots, M\}$  do
    if  $B_p \times S_i(\{\{1, \dots, M\}, \{\phi\}\}) \geq B_s \times S_i(\{\{\phi\}, \{1, \dots, M\}\})$  then
       $\mathcal{U}^{(p)} \leftarrow \mathcal{U}^{(p)} \cup \{m\}$ 
    else
       $\mathcal{U}^{(s)} \leftarrow \mathcal{U}^{(s)} \cup \{m\}$ 
    end if
  end for
   $R \leftarrow \sum_{r=1}^2 \sum_{i \in \mathcal{U}^{(p_r)}} R_i^{(p_r)} + \sum_{j \in \mathcal{U}^{(s)}} R_j^{(s)}$ 
  if  $R > R^*$  then
     $R^* \leftarrow R$     % Updating the max inter-RAN sum rate
     $\mathcal{B}^* \leftarrow \{0.5B(K - k)/K, Bk/K\}$     % Updating the best  $\mathcal{B}$ 
     $\mathcal{U}^* \leftarrow \{\{\mathcal{U}^{(p)}\}, \{\mathcal{U}^{(s)}\}\}$     % Updating the best  $\mathcal{U}$ 
  end if
end for

```

6 Simulation Results and Analysis

In this chapter, several system level simulation results are used to show the performance improvement gain that could be achieved from the proposed dynamic spectrum allocation in co-located RANs (refer Chap. 5). The RANs are assumed to be owned by separate operators. In addition, as a baseline for comparison, simulations are also made for two extreme cases. In the first case, the total available spectrum for the RANs is equally partitioned and dedicatedly allocated to each operator. The BSs in each RAN are assumed to jointly serve their users using zero forcing precoding with a sum rate and equal per stream power constraint. In the second case, the whole available spectrum for the RANs is shared in a non-orthogonal way among the operators. The BSs of each RAN are assumed to implement sparse precoding to minimise inter-operator interference with the merely exchange of CSI.

6.1 Simulation Scenario

6.1.1 Network Layout

We considered a network layout shown in Fig. 16 where the two co-located C-RANs are owned by two operators. Each C-RAN is assumed to have four RRH. The RRHs

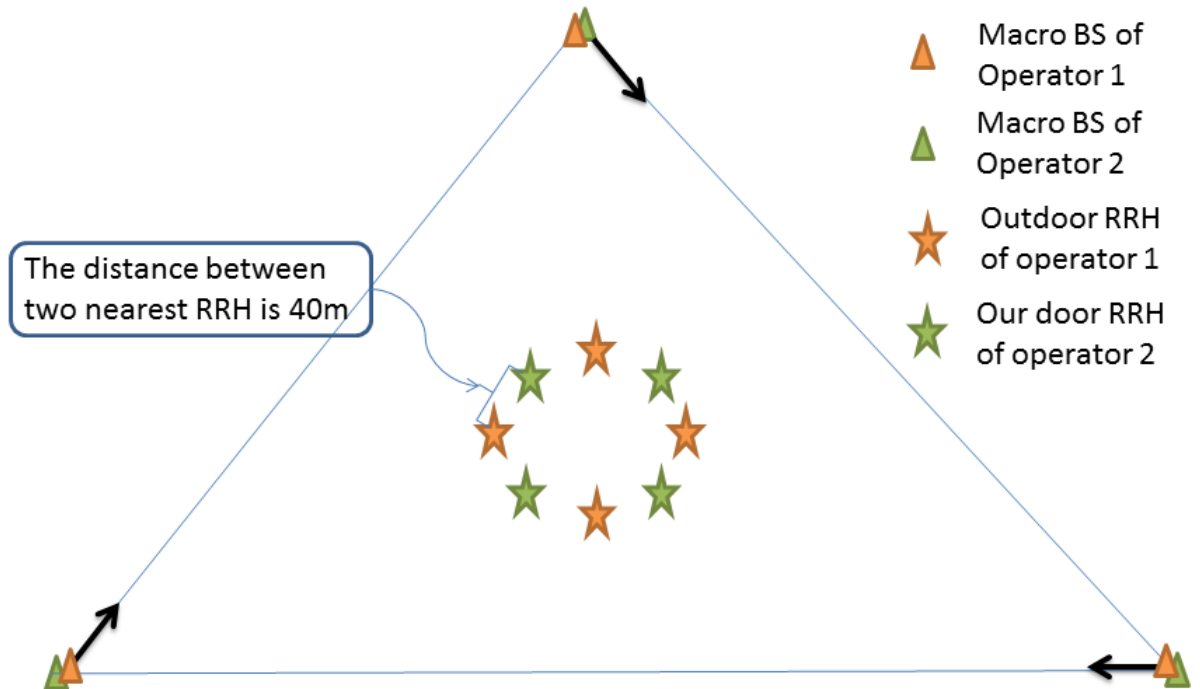


Figure 16: Illustration of the simulated network layout. Two co-located C-RANs each consisting of 4 RRHs are considered. The macrocells of each operator share the same towers.

of both C-RANs are arranged such that the users of both C-RANs will have the same probability of getting useful and interference signal when uniformly distributed in a circle having the same center as the center of RRH coordinates. In addition, the distance between two nearest RRH is taken to be 40m, which is the minimum separation distance requirement by 3GPP. Moreover, each RRH is assumed to be connected to the central processing unit using fiber optics, which makes it suitable to apply joint transmission. Furthermore, we assume that the two cloud RAN systems are connected with fiber optics for the purpose of exchanging CSI and control information.

On the other hand, the six macrocells are included in order to consider the effect of external interference from other cell layers. A user is likely to experience such kind of external interference especially in heterogeneous network, which at this time is becoming popular. In order to create a symmetric external interference from the macrocells, they are arranged such that they have the same center of points as the RRHs. In addition, the two operators are assumed to share the same tower for their macrocell coverage. Moreover, the inter-site distance of the macrocells is used to adjust the strength of the external interference on the users. Therefore, as the inter-site distance decreases, the strength of the external interference increases.

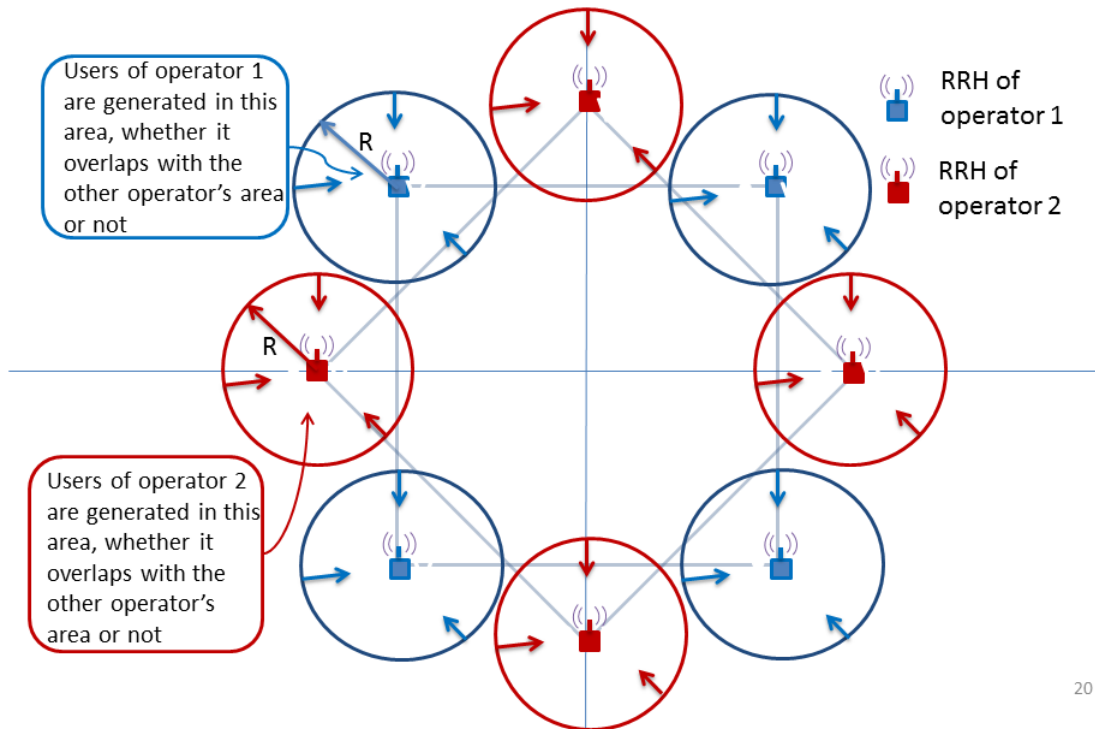


Figure 17: Illustration of 'User Distribution Type-I'. In this case, a user of an RRH is uniformly distributed within a radius R from the RRH.

6.1.2 User Distribution

It is assumed that only a single user is served per RRH, in accordance with the assumption taken in Chap. 5. Three user distribution types are considered for different purposes. In the first user distribution type, which we label it as 'user distribution type-I', the user of a given operator is uniformly distributed within a radius R meters from its anchor RRH as shown in Fig. 17. This type of distribution could, for example, help us study if the users which are found near their own RRH could be benefited if served in the shared frequency sub-band.

The second type of user distribution, which we label is as 'user distribution type-II', is show in Fig. 18. In this case, a user is uniformly distributed within radius R meters of the big circle, except it is not allowed within radius r meters of the other operator's RRH. This type of user distribution is introduced in order to indirectly study the behaviour of the users which are located in the vicinity of the other operator's RRH, that is, the interfering RRH if the user is being served in the shared bandwidth.

The third type of user distribution, which we label it as user distribution type-III, is show in Fig. 19. In this type of user distribution, all the users are uniformly distributed within radius R meters of the circle. This type of user distribution is introduced to study of the average performance of the users.

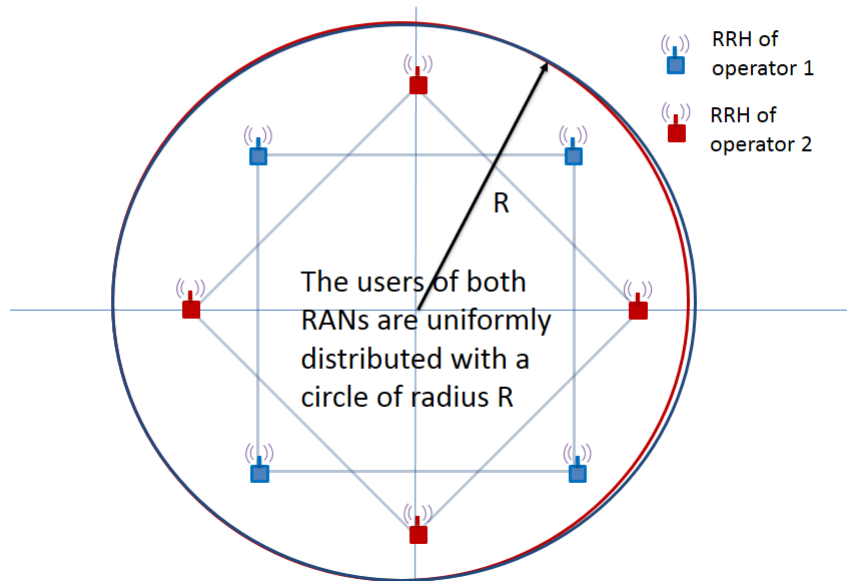


Figure 18: Illustration of 'User Distribution Type-II'. all the users of both operators are uniformly generated within radius R from the center of the RRHs coordinates. The size of R could be large enough to encompass all the RRHs.

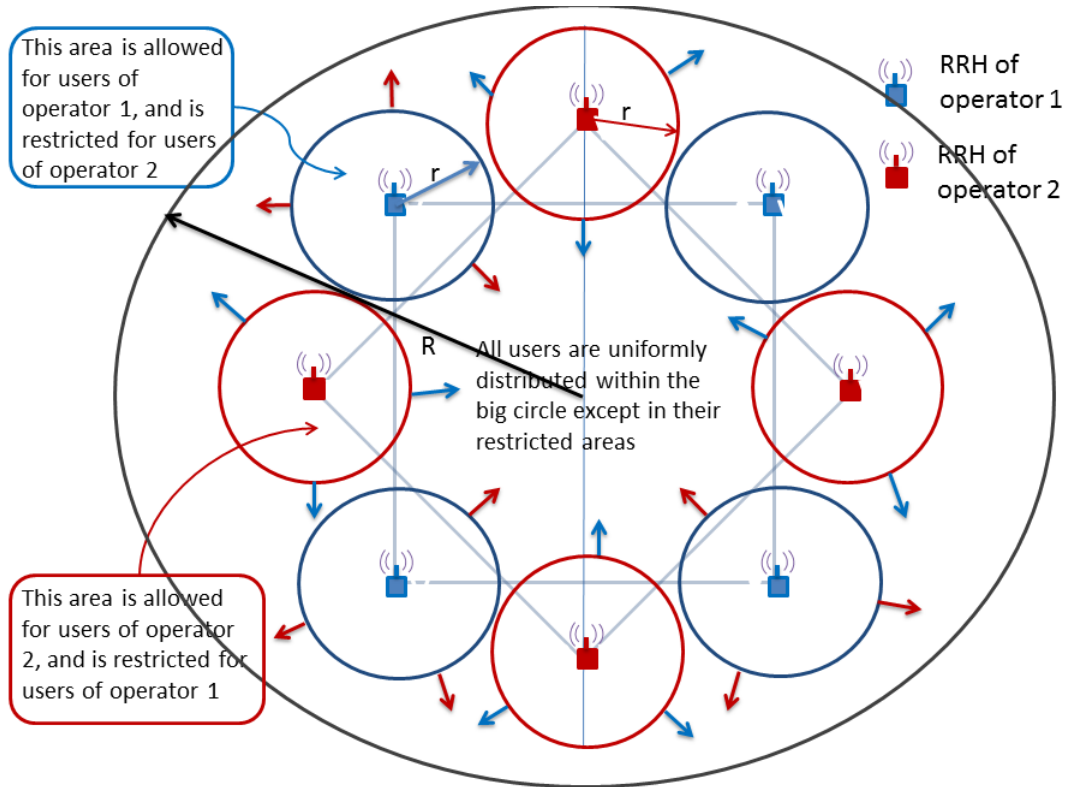


Figure 19: Illustration of 'User Distribution Type-III'. Users of all operators are uniformly generated within radius R from the center of the RRH coordinates. However, users of operator 1 are not allowed to be generated within radius r of operator 2's RRHs, and vice versa.

6.2 Simulation Parameters and Models

6.2.1 Simulation Parameters

We can assume the considered network layout as an LTE's heterogeneous network which consists of macrocells and RRHs. Therefore, the standard for LTE network simulations is used. As mentioned in [49], the simulation parameters are summarised in Table 1. We further assume that the two operators are allocated with a **BW! (BW!)** of 5 MHz each and their center frequencies are chosen to be adjacent. However, the center of frequencies of the operators need not be adjacent. For example, if we assume the UEs are LTE-release 10 users, then carrier aggregation can be applied to serve the users in the shared frequency sub-band if the bandwidth of the operators is not contiguous.

6.2.2 Antenna Pattern

Antenna pattern is used to define the dependency of the strength of the transmitted radio signal on the direction of the receiver with respect to the transmitter. In our case, the RRHs are assumed to be omnidirectional, while for the macrocells, a 3D


Parameter	Value used for evaluation
Network layout	As in section 6.1.1
Carrier frequency	1997.5 MHz (of operator 1)
	2002.5 MHz (of operator 2)
Bandwidth	10 MHz per operator
Macrocell Tx power	43 dBm per 5 MHz carrier
RRH Tx power	27 dBm per 5 MHz carrier
Macrocell antenna gain including cable losses	15 dB
RRH antenna gain including cable losses	5 dB
UE noise figure	5 dB
Antenna bore sight	
UE distribution	As in section 6.1.2
Distance dependent pathloss model	As in section 6.2.3
Fading model	As in section 6.2.3
Macrocell antenna pattern	As in section 6.2.2
RRH antenna pattern	Omnidirectional

Table 1: Simulation parameters

model is used where the strength of the transmitted signal depends on both the horizontal and vertical directions.

Accordingly, the horizontal antenna pattern is given as

$$A_H = -\min\left[12\left(\frac{\varphi}{\varphi_{3dB}}\right)^2, A_m\right] \quad (34)$$

$$\varphi_{3dB} = 70, A_m = 25dB$$

Similarly, the vertical antenna pattern is given as

$$A_V = -\min\left[12\left(\frac{\theta - \theta_{\text{etilt}}}{\theta_{3dB}}\right)^2, SLA_v\right] \quad (35)$$

$$\theta_{3dB} = 10, SLA_v = 20dB$$

For the simulation scenario that we are considering, that is, a heterogeneous network with outdoor RRHs, a value of $\theta_{\text{etilt}} = 15$ degrees is taken.

6.2.3 Channel Model

In wireless communication, the received signal in time domain, $y(t)$, can be expressed mathematically as

$$y(t) = h(t)x(t) + n(t) \quad (36)$$

where $x(t)$ is the transmitted signal, $h(t)$ is the channel response, and $n(t)$ is the thermal noise.

The noise, $n(t)$, is modelled as additive white Gaussian noise. Whereas, several effects of the wireless channel, such as pathloss, shadowing (large scale) fading, and multipath (small scale) fading, are included in the channel response, $h(t)$, and different models are used for modelling each effects. The pathloss is used to model the distance dependent attenuation incurred by the wireless channel on the transmitted signal. Several theoretical, physical and statistical models exist to model the effect of pathloss. In our case, we use the standard statistical models used by 3GPP as mentioned in [49]. Accordingly, the distance dependent pathlosses from macrocell to a UEs and RRHs to UE are given as follows:

Macrocell to UE

$$L = 128.1 + 37.6 \log_{10}(R) \quad (37)$$

RRH to UE

$$L = 140.7 + 37.6 \log_{10}(R) \quad (38)$$

where L denotes the distance dependent pathloss, R is in km and denotes the distance between the transmitter and receiver.

Multipath fading occurs as a result of the delayed arrival of the transmitted signal due to multiple scatterers such as buildings, trees, and other structures. In big cities, the angle of arrival of the signal is assumed to be uniformly distributed between 0 and 2π . Those signals which arrive at the same time may thus add up either constructively or destructively depending on their phase. In general, when there is no dominant line of sight, the amplitude of the received signal is modelled to follow Rayleigh distribution. Accordingly, we use the Rayleigh fading model to generate the multipath fading channels.

6.3 Performance Assessment Method

The data rate of the users is taken as the performance measurement metric. The data rate of the users is calculated according to equations 30 and 31, depending whether the user is served in the private or shared frequency sub-bands, respectively. In this case, the thermal noise and external interference from the macrocell layer experienced by a user depends on the amount of bandwidth allocated for private or orthogonal sub-bands depending on which sub-band is the user served. In general,

the average user data rate is calculated as the sum of the data rates of all users of both operators divided by the total number of the users.

6.4 Comparison of Orthogonal and Full spectrum Allocations

Before we go to the simulation of the performance of the dynamic spectrum allocation, we first compare the performance of two extreme bandwidth allocation schemes, the conventional way of allocating orthogonal bandwidth to both operators, which we call it 'orthogonal spectrum allocation', and the aggressive way of allocating the whole spectrum to both operators, which we label it 'full spectrum allocation'. Both spectrum allocations have their own advantages and disadvantages. When we use orthogonal spectrum allocation, there is no inter-operator interference. Nevertheless, this is done at the cost of allocating only half of the available spectrum to each operators in order to keep orthogonality among them. when full spectrum allocation is used, the whole spectrum used by both operators. However, this lead to inter-operator interference. In addition, the interference from macrocell layer and thermal noise on a user served with full spectrum allocation are doubled when compared to quantities if that user was served using orthogonal spectrum allocation.

The main aim of this Section is to analyse whether one of the spectrum allocations could be dominant over the other under all situations. If none of the spectrum allocation schemes is always dominant, the conditions under which each spectrum allocation is better than the other is analysed. These comparisons are carried out under the three user distribution types.

6.4.1 User Distribution Type-I

In this subsection, the performance of the users under orthogonal and full spectrum allocations are compared when the users are distributed using user distribution type-I. The simulation result is plotted as average user rate versus the radius R , which is the radius of the circle in which the user of a given RRH is uniformly distributed. According to Fig. 20, when the inter-site distance of the macrocells is low, the users have better performance of when served under full spectrum allocation than orthogonal spectrum allocation. In other words, full spectrum allocation has better performance than orthogonal spectrum allocation in high external interference situation.

However, when the Inter-site Distance (ISD) of the macrocells increase, that is, when the external interference decreases, the performance of full spectrum allocation increases until finally becomes interference limited due to the internal interference from other RRHs. Whereas the performance of orthogonal spectrum allocation increase until becomes noise limited. Therefore, at low external interference, the performance of orthogonal spectrum allocation outperforms the performance of full

spectrum allocation.

on the other hand, in situation where the performance of full spectrum allocation is better, the performance improvement is higher for lower values of R . This implies, the users which are found near their RRH are more beneficial with spectrum sharing than those which are found far away. This is reasonable, as the users which are found near their serving RRH are likely to face an interference with much lower strength when compared to the strength the useful signal. Thus the performance improvement they would get with the use of higher bandwidth would outperform the loss they would incur due to inter-operator interference. Finally, we observe that as the radius R increases, the performance of both full and orthogonal spectrum allocations decrease. This is due to the reason that, on average, the received signal become weaker as R increases due to pathloss.

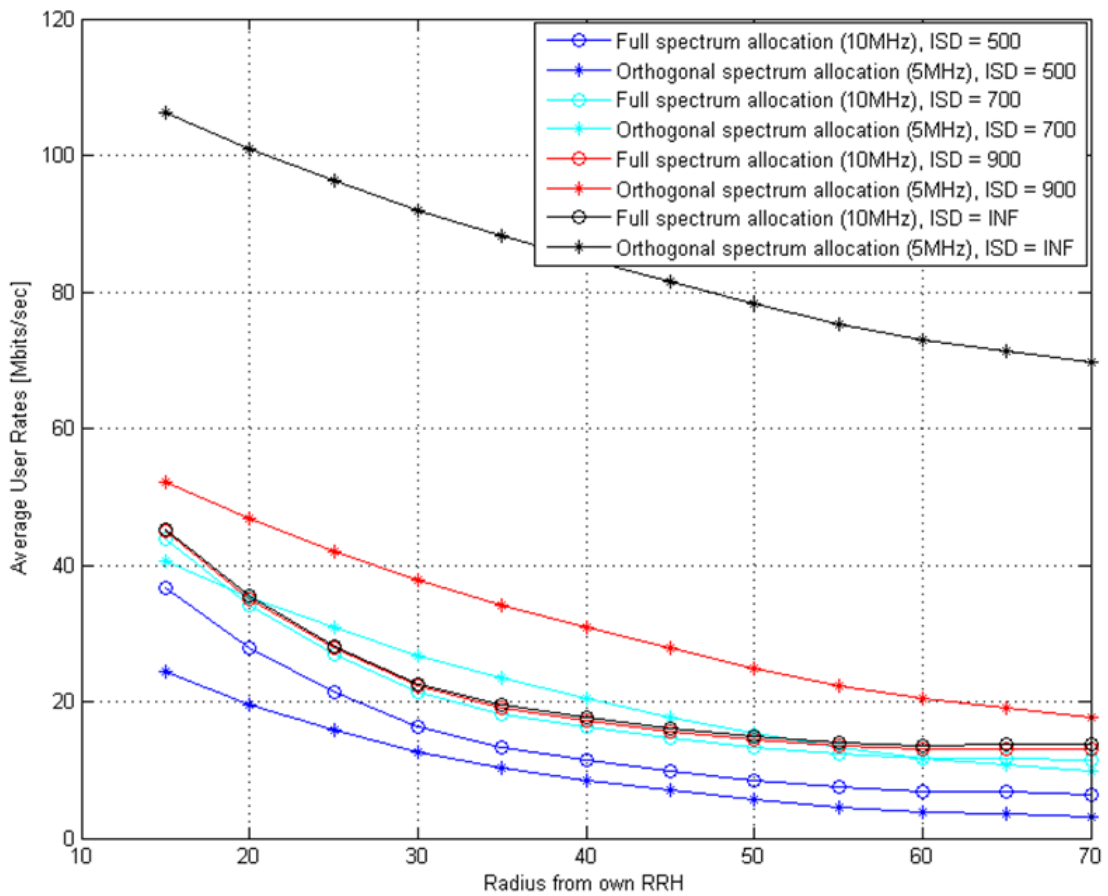


Figure 20: Comparison of orthogonal vs full spectrum allocations with user distribution type-I

6.4.2 User Distribution Type-II

In this subsection, the performance of the users under orthogonal and full spectrum allocations are compared when the users are distributed using user distribution type-II. The simulation result is plotted as average user rate versus the radius R , which is the radius of the circle centred at the center of points of the RRHs. Similar results are shown in Fig. 21 as in Fig. 20. As the external interference decreases, the performance of full spectrum allocation increases, but quickly becomes limited to the internal interference from other RRHs. Whereas the performance of orthogonal spectrum allocation increases until becomes noise limited. In addition, at high external interference, the performance of full spectrum allocation outperforms the performance of orthogonal spectrum allocation. Whereas, the opposite happens at low external interference.

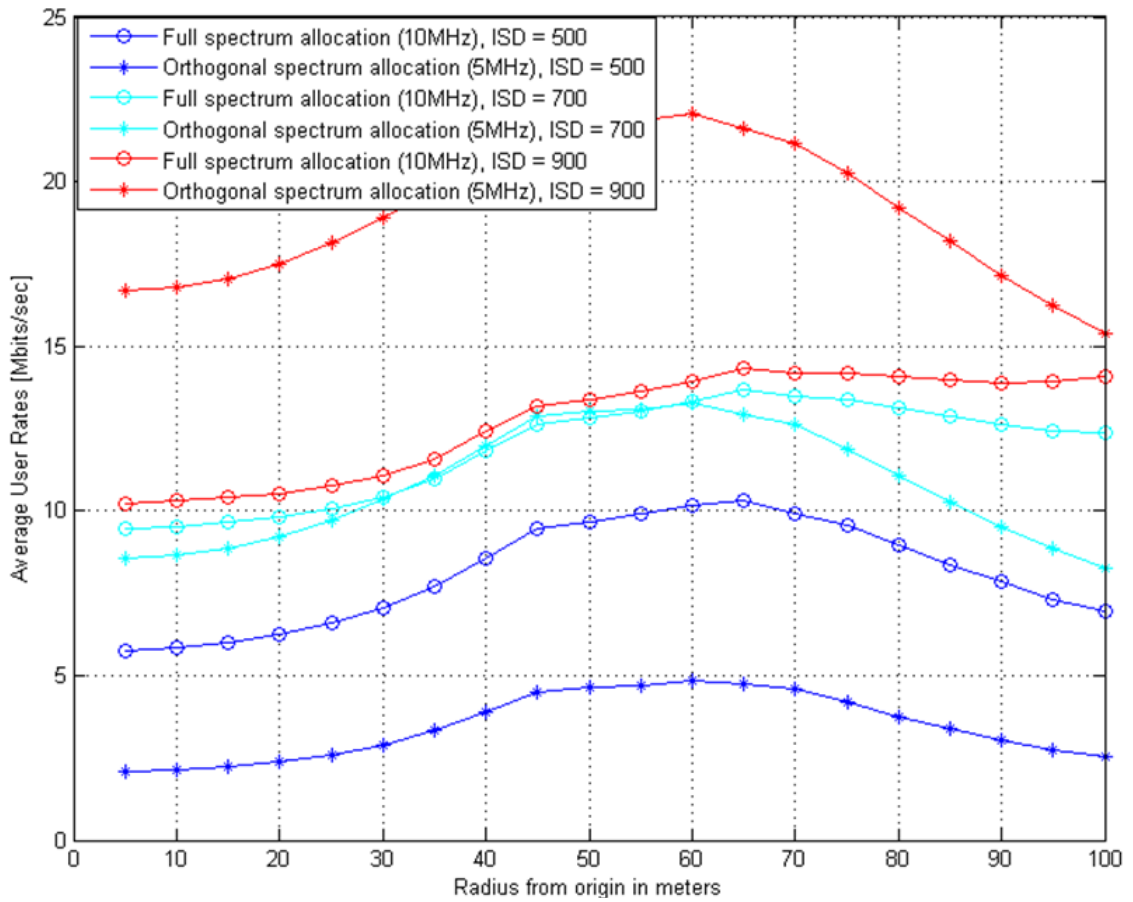


Figure 21: Comparison of orthogonal vs full spectrum allocations with user distribution type-II

6.4.3 User Distribution Type-III

In this subsection, the performance of the users under orthogonal and full spectrum allocations are compared when the users are distributed using user distribution type-III. The simulation result is plotted as average user rates versus the radius r , which is the radius of the circle inside which the users of the other operator are not allowed to be generated. The larger radius R is fixed to be 65m, with the aim of choosing a radius which gives the highest performance for the users from Fig. 21.

Similar to Fig. 20 and Fig.21, as the external interference decreases, the performance of full spectrum allocation increases, but quickly becomes limited to the internal interference from other RRHs. Whereas the performance of orthogonal spectrum allocation increases until becomes noise limited. In addition, at high external interference, the performance of full spectrum allocation outperforms the performance of orthogonal spectrum allocation. Whereas, the opposite happens at low external interference. But additionally, as the the size of the forbidden area, that's the value

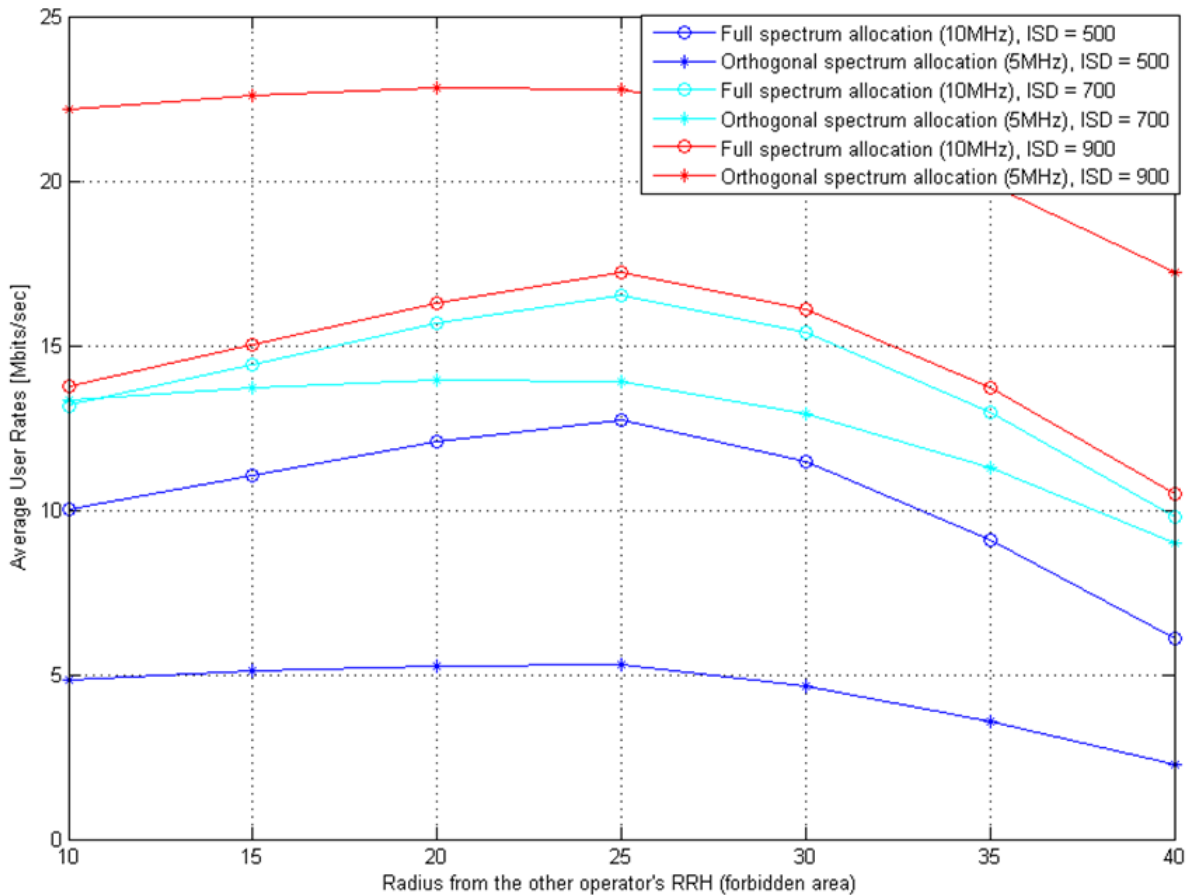


Figure 22: Comparison of orthogonal vs full spectrum allocations with user distribution type-III

of r , increases, the performance of full spectrum allocation increases. This shows forcing the users which are found in the vicinity of the other operators RRH, which in this case is an interfering RRH, to be served in a shared bandwidth makes the users suffer from strong interference which in turn results in an overall performance degradation.

6.5 Performance of Dynamic Spectrum Allocation

In Sec. 6.4, we have compared the performance of orthogonal and full spectrum allocation. As we have seen from the simulation results, neither orthogonal nor full spectrum allocation are dominant under all situations. Besides, users which are found near their serving RRH generally prefers full spectrum allocation whereas those found in the vicinity of the interfering RRH prefers orthogonal spectrum allocation. In this section, the performance of a dynamic spectrum allocation which is implemented using the proposed heuristic algorithm based on user grouping (refer to Sec. 5.2.2) is simulated. In the simulations, the parameter $K = 10$ is used, that

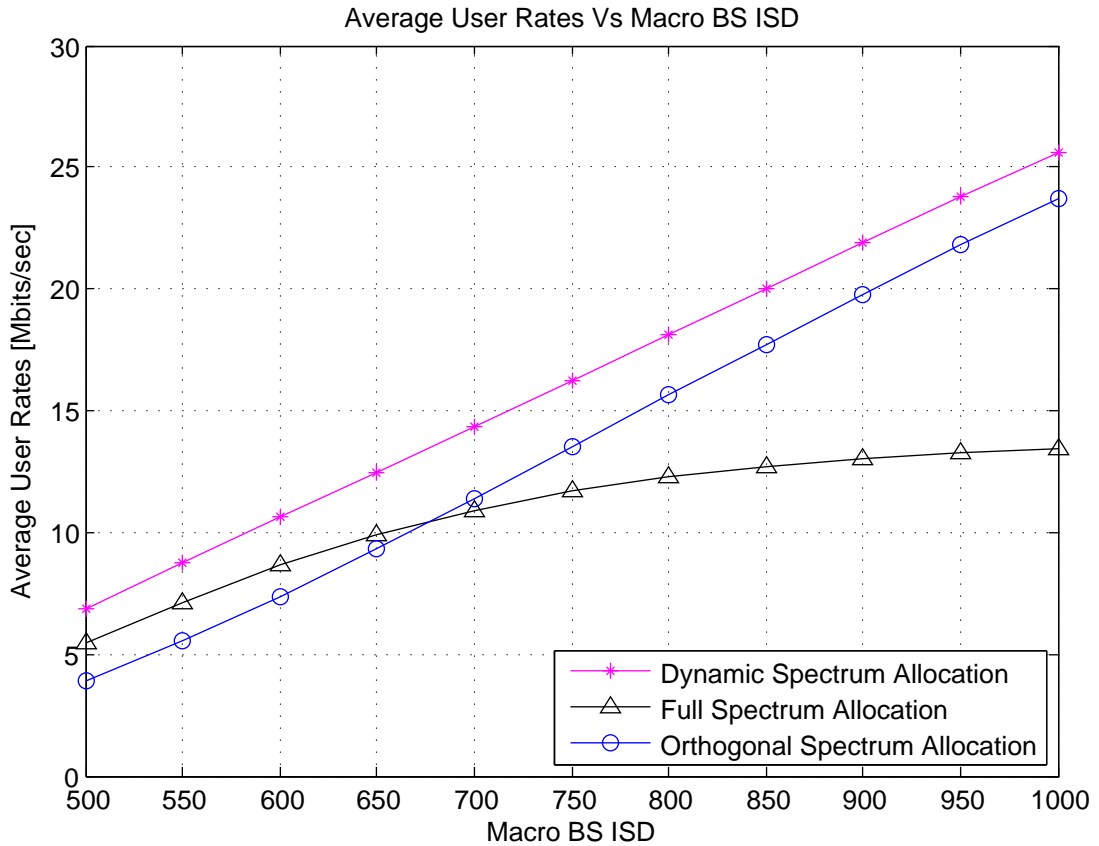


Figure 23: Performance of dynamic spectrum allocation is compared with orthogonal and full spectrum allocations under User Distribution Type-I with parameter $R = 60\text{m}$.

is, the minimum bandwidth that can be allocated is W/K , where W is the total bandwidth available for both operators. For each fast fading realization, the best among the 11 possible bandwidth allocations is chosen according to Sec. 5.2.2.

As the simulation results in Fig. 23, Fig. 24 and Fig. 25 show, the performance of dynamic spectrum allocation is always better than orthogonal or full spectrum allocation. This results directly comes from the nature of the heuristic algorithm as it always chooses the allocation with the best inter-RAN sum rate among the set of candidate spectrum allocations and both the orthogonal and full spectrum allocations are a member of this set. But, in addition, the heuristic algorithm helps the users to be served in their preferred frequency sub-band (private or shared frequency sub-band), and the overall performance of all the users is improved. On the other hand, the performance improvement with the dynamic spectrum allocation is significant at lower macrocell inter-site distance, that is, at lower external interference. The main reason for this is that the region within the network where the inter-operator interference is negligible when compare to the sum of back ground

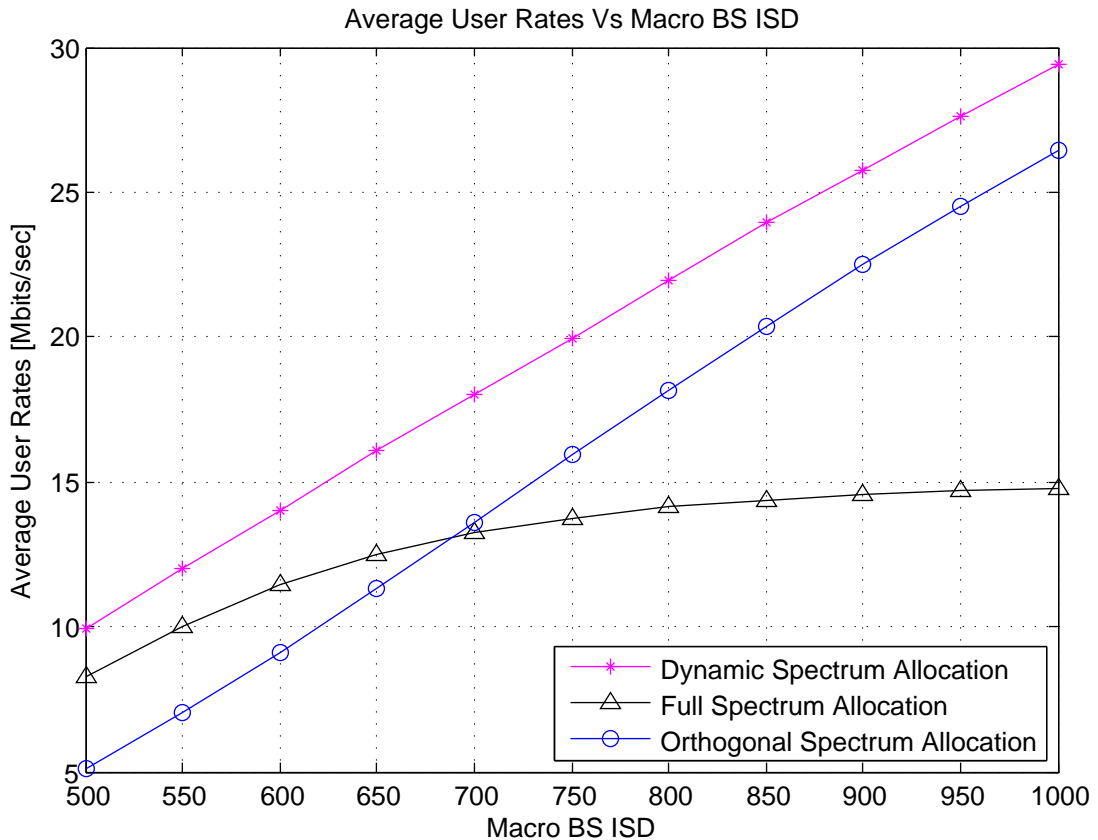


Figure 24: Performance of dynamic spectrum allocation is compared with orthogonal and full spectrum allocations under User Distribution Type-II with parameter $R = 65\text{m}$.

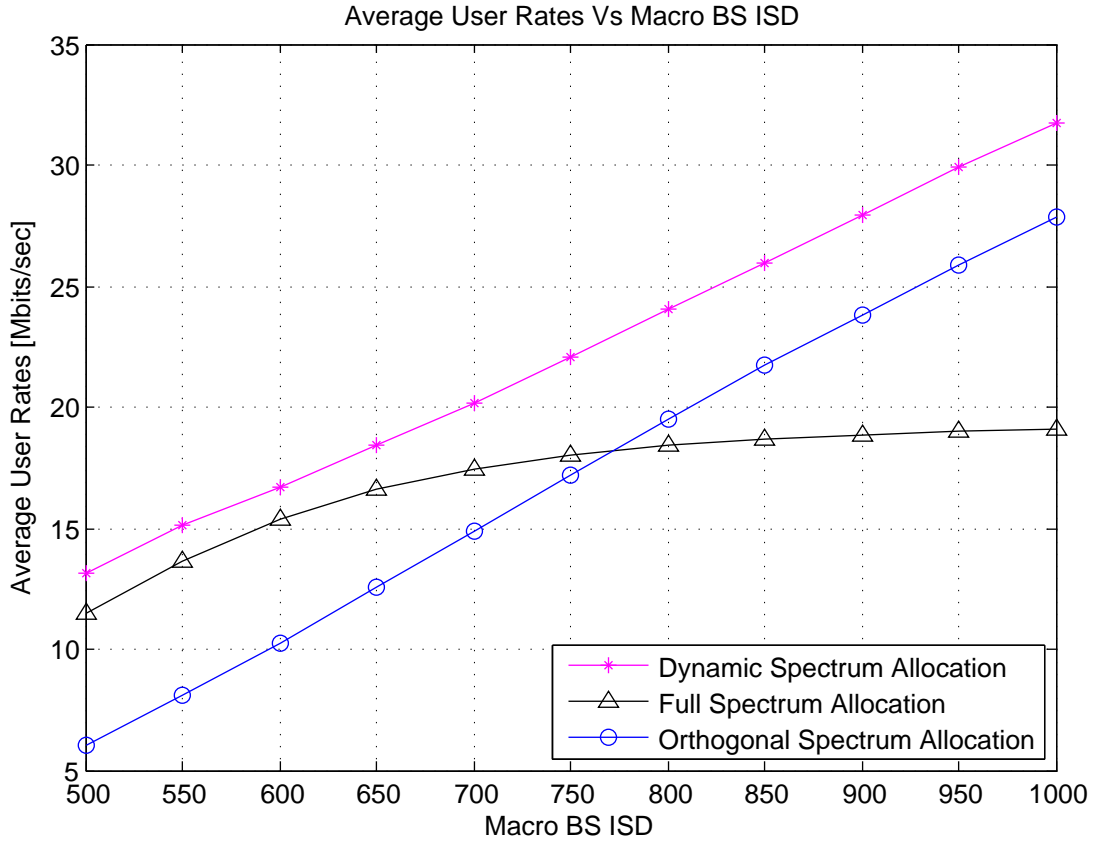


Figure 25: Performance of dynamic spectrum allocation is compared with orthogonal and full spectrum allocations under User Distribution Type-III with parameters $R = 65\text{m}$ and $r = 25\text{m}$.

noise and external interference increases as the strength of the external interference increases. Therefore, the region where the same frequency resource can be safely reused among the operators increases leading to better overall performance. Using similar argument, it can be justified that as the external interference decreases, the performance improvement decreases.

7 Conclusion and Future Work

The problem of adaptive inter-operator spectrum sharing between co-located RANs is studied in this thesis. For this purpose, an efficient approach for adaptive inter-operator spectrum sharing is proposed and explained. In this approach, the available spectrum is partitioned into private and shared frequency sub-bands. Each operator serves some of its users in its private frequency sub-band, while the rest of the users in the shared frequency sub-band, implementing inter-operator interference coordination. In addition, a heuristic algorithm based on user grouping is proposed for finding the best spectrum partition with the aim of maximizing inter-RAN interference. Besides, the partitioning of the spectrum is adapted based on the channel condition of the users.

For the purpose of performance analysis of the proposed adaptive inter-operator spectrum sharing approach, a scenario with two co-located C-RANs is taken. In addition, a macrocell layer is introduced in the scenario for the purpose of analyzing the effect of external interference on the performance. Moreover, equal number of UEs and RRH is used. As a baseline for comparison, two cases of spectrum allocation approaches were considered: orthogonal and full spectrum allocations. In orthogonal spectrum allocation, the available spectrum is partitioned into two exclusive orthogonal sub-bands which are allocated to each operator. In full spectrum allocation, the whole available spectrum is shared in a non-orthogonal way among the RANs minimizing inter-RAN interference.

7.1 Conclusion

Based on simulation results from the comparison of the performance of orthogonal and full spectrum allocations, it can be observed that neither of the allocations is better than the other under all situations. For example, in situation where there is strong external interference, full spectrum allocation outperforms orthogonal spectrum allocation in-terms of average inter-RAN sum data rate. The opposite happens when there is weak or no external interference. Therefore, it can be concluded that the performance of orthogonal and full spectrum allocations can be improved if they are simultaneously applied in different regions of the network (for different groups of users) - as it is done in the proposed adaptive spectrum sharing approach.

As it is shown from simulation results, the proposed adaptive spectrum sharing approach outperforms the orthogonal and full spectrum allocation approaches under all situations. It is shown that the gain comes first from the fact that the scheme tries to serve UEs in accordance with their best option with regard to achieving higher UE data rate. Second, both orthogonal and full spectrum allocations are a member of the set of spectrum allocations from which the best allocation is chosen in-terms of inter-RAN sum rate. In addition, it is shown that the gain of the adaptive spectrum sharing approach over orthogonal spectrum allocation increases as external interference increases. This accounts for the fact that the area where

inter-operator interference is insignificant when compared to the background noise (external interference plus thermal noise) increases as the external interference increases.

7.2 Future Work

There are several areas where the research work in this thesis could be expanded. In the thesis, a greedy approach was used to maximise inter-RAN sum rate. However, fairness among the users could also be included in the optimisation problem by rather maximising a sum of a utility function of the rates. In addition, it is assumed that there exist perfect CSI. Yet, the channel estimation and feedback capability of the UEs could be taken into consideration to have more practical assumptions. Moreover, a more computational demanding and non ad-hoc approach could be used when grouping the users for a fixed spectrum partition. These could be incorporated in the thesis work or its extensions mentioned below. Directions of future work are suggested as follows:

1. In the thesis, only equal number UEs and BSs with a flat fading channel model is used in order to avoid the problem of OFDM scheduling. Extending the work to a multi-user per BS scenario with frequency selective fading channel model could lead to interesting results. In such scenario, multi-user diversity could be exploited for creating additional gains. In addition, the partition of the spectrum (into private and shared spectrum sub-bands) could be done based on long term measurements and slowly adapted due to availability of large number of users. However, the problem of OFDM scheduling could be challenging.
2. Increasing the number of cooperating operators is another possible extension work. Considering K number of cooperating operators, there will be regions in the network where a frequency resource can be simultaneously used by upto K operators with insignificant or controllable inter-operator interference. Therefore, this could lead to a significant performance improvement. However, finding regions in the network coverage where each possible combinations of operators reusing the same resource with manageable inter-operator interference is challenging. Additionally, finding combination of users which will be classified as users of these regions is challenging as well.
3. Applying the proposed or other adaptive inter-operator spectrum sharing schemes among RANs covering a wide range of area could be difficult. Therefore, creating clusters of BSs within the RANs of each operator and implementing the scheme among co-located clusters of BSs belonging to different operators could be a good idea in terms of reducing the requirement on backhaul network capacity and latency. In this case, the problem of BS clustering combined with the problem of efficiently sharing the spectrum could be challenging.

References

- [1] Nokia Siemens, *Wake-up call: Industry collaboration needed to make Beyond 4G networks carry 1000 times more traffic by 2020*, White Paper, August 2011, Available: <http://blogs.nokiasiemensnetworks.com/news/2011/08/24/beyond-4g-networks/>
- [2] Ericsson, *More than 50 billion connected devices*, White Paper, February 2011, Available: <http://www.ericsson.com/res/docs/whitepapers/wp-50-billions.pdf>
- [3] S. M. Blust.(2012). *IMT-Advanced standards for mobile broadband communications* [Online]. Available: <http://www.itu.int/net/newsroom/wrc/2012/features/imt.aspx>
- [4] H. Holma and A. Toskala, *LTE for UMTS - Evolution to LTE Advanced*, 2nd ed., Wiley, 2011.
- [5] S. Liu, et al, *A 25 Gb/s(/Km²) Urban Wireless Network Beyond IMT-Advanced*, IEEE Commun. Mag., vol. 49, n. 2, pp. 122-129, February 2011.
- [6] Estimated spectrum bandwidth requirements for the future development of IMT-2000 and IMT-Advanced.
- [7] E. G. Larson and E. A. Jorswieck, *Competition versus cooperation on the MISO interference channel*, IEEE J. Sel. Areas Commun., vol. 26, n. 7, pp. 1059-1069, September 2008.
- [8] L. Anchora, L. Canzian, L. Badia, and M. Zorzi, *A Characterization of Resource Allocation in LTE Systems Aimed at Game Theoretical Approaches*, IEEE CAMAD, pp. 47-51, December 2010.
- [9] Jian Luo, Johannes Lindblom, Jianhui Li, Rami Mochaourab, Andreas Kortke, Eleftherios Karipidis, Martin Haardt, Eduard A. Jorswieck, Erik G. Larsson: *Transmit Beamforming for Inter-Operator Spectrum Sharing: From Theory to Practice*, IEEE ISWCS, pp. 291-295, August 2012.
- [10] Bennis M, Lasaulce S and Debbah M, *Inter-operator spectrum sharing from a game theoretical perspective*, EURASIP Journal on Advances in Signal Processing, September 2009.
- [11] P. de Kerret and D. Gesbert, *Sparse Precoding in Multicell MIMO Systems*, IEEE WCNC, pp. 958-62, April 2012.
- [12] ITU-R, *Invitation for submission of proposals for candidate radio interface technologies for the terrestrial components of the radio interface(s) for IMT-advanced and invitation to participate in their subsequent evaluation*, ITU-R SG5, Circular Letter 5/LCCE/2, March 2008.
- [13] ITU-R M.[IMT-TECH] *Requirements related to technical performance for IMT-Advanced radio interface(s)*, August 2008.

- [14] [Online] Available: <http://www.profheath.org/research/heterogeneous-networks/>
- [15] China Mobile Research Institute, *C-RAN – The Road Towards Green RAN*, White Paper, April 2010.
- [16] A. Banerjee, Y. Park, F. Clarke, H. Song, S. Yang, G. Kramer, K. Kim, B. Mukherjee, *Wavelength-division-multiplexed passive optical network (WDM-PON) technologies for broadband access: a review*, Optical Society of America, Journal of optical Networking, vol. 4, no. 11, 2005.
- [17] A. F. Molisch, *Wireless Communications*. Wiley-IEEE Press, 2005.
- [18] H. Zhang, B. Mehta, F. Molisch, J. Zhang, and H. Dai, *Asynchronous Interference Mitigation in Cooperative Base Station Systems*, IEEE Trans. Wireless Commun., vol. 7, no. 1, pp. 155-156, May 2007.
- [19] D. Gesbert, S. Hanly, H. Huang, S. Shamai Shitz, O. Simeone, and W. Yu, *Multi-Cell MIMO Cooperative Networks: A New Look at Interference*, IEEE J Sel. Areas Commun., vol. 28, no. 9, pp. 1380-1408, December 2010.
- [20] F. Xiangning, C. Si, Z. Xiaodong, *An Inter-cell Interference Coordination Technique Based on Users' Ratio and Multi-Level Frequency Allocations*, IEEE WiCom, pp. 799-802, September 2007.
- [21] Y. Chang, Z. Tao, J. Zhang, C. Kuo, *A Graph Approach to Dynamic Fractional Frequency Reuse (FFR) in Multi-Cell OFDMA Networks*. In *Communications*, IEEE ICC, pp. 1-6, June 2009.
- [22] L. Chen, D. Yuan, *Generalizing FFR by flexible sub-band allocation in OFDMA networks with irregular cell layout* IEEE WCNC, pp. 1-5, April 2010.
- [23] D. Gesbert, M. Shafi, P. Smith, D. Shiu, and A. Naguib, *From Theory to Practice: An overview of MIMO space-time coded wireless systems*, IEEE J Sel. Areas Commun., vol. 21, no. 3, pp 281-302, April 2003.
- [24] F. Akyildiz, M. Gutierrez, C. Reyes, *The evolution to 4G cellular systems: LTE-Advanced*, Elsevier J. of Physical Commun., vol. 3, no. 4, pp. 217-244, December 2010.
- [25] CELTIC/CP5-026 WINNER+, *D1.4 initial report on advanced multiple antenna systems*, Tech. Rep., January 2009.
- [26] A. Papadogiannis, H.J. Bang, D. Gesbert, E. Hardouin, *Downlink overhead reduction for multi-cell cooperative processing enabled wireless networks*, IEEE PIMRC, pp. 1-5, September 2008.
- [27] C. Ng and H. Huang, *Linear Precoding in Cooperative MIMO Cellular Networks with Limited Coordination Clusters*, IEEE J. Sel. Areas Commun., vol.28, no.9, pp. 1446-1454, December 2010.

- [28] O. Simeone, O. Somekh, H. Poor, and S. Shamai (Shitz), *Downlink Multicell Processing with Limited Backhaul Capacity*, EURASIP Journal on Advances in Signal Processing, May 2009.
- [29] L. Venturino, N. Prasad, and X. Wang, *Coordinated scheduling and power allocation in downlink multicell OFDMA networks*, IEEE Trans. Veh. Technol., vol. 58, no. 6, pp. 2835-2848, July 2009.
- [30] A. Leshem and E. Zehavi, *Cooperative game theory and the Gaussian interference channel*, IEEE J. Selec. Areas Commun., vol. 26, no. 7, pp. 1078-1088, September 2008
- [31] W. Yu, T. Kwon, and C. Shin, *Joint scheduling and dynamic power spectrum optimization for wireless multicell networks*, IEEE CISS, pp. 1-6, March 2010
- [32] H. Dahrouj and W. Yu, *Coordinated beamforming for the multicell multi-antenna wireless system*, IEEE Trans. Wireless Commun., vol. 9, no. 5, pp. 1748-1759, May 2010.
- [33] H. Dahrouj and W. Yu, *Interference mitigation with joint beamforming and common information decoding in multicell systems*, IEEE ISIT, pp. 2068-2072, June 2010.
- [34] M. Karakayali, G. J. Foschini, and R. A. Valenzuela, *Network coordination for spectrally efficient communications in cellular systems*, IEEE Wireless Commun., vol. 13, no. 4, pp. 56-61, August 2006.
- [35] S. Shamai and B. M. Zaidel, *Enhancing the cellular downlink capacity via co-processing at the transmission end*, IEEE VTC, pp. 1745-1749, May 2001.
- [36] S. Jafar, G. Foschini, and A. Goldsmith, *Phantomnet: Exploring optimal multicellular multiple antenna systems*, EURASIP Journal on Applied Signal Processing, pp. 591-604, January 2004.
- [37] C. Windpassinger, R. F. H. Fischer, T. Vencel, and J. B. Huber, *Precoding in multi-antenna and multiuser communications*, IEEE Trans. Wireless Commun., vol. 3, no. 4, pp. 1305-1316, July 2004.
- [38] H. Dai, A. F. Molisch, and H. V. Poor, *Downlink capacity of interference-limited MIMO systems with joint detection*, IEEE Trans. Wireless Commun., vol. 3, no. 2, pp. 442-453, March 2004.
- [39] J. Zhang, Y. Wu, S. Zhou, and J. Wang, *Joint linear transmitter and receiver design for the downlink of multiuser MIMO systems*, IEEE Commun. Lett., vol. 9, no. 11, pp. 991-993, November 2005.
- [40] A. Tarighat, M. Sadek, and A. H. Sayed, *A multiuser beamforming scheme for downlink MIMO channels based on maximizing signal-to-leakage ratios*, IEEE ICASSP, pp. 1129-1132, March 2005.

- [41] H. Zhang and H. Dai, *Cochannel interference mitigation and cooperative processing in downlink multicell multiuser MIMO networks*, EURASIP Journal on Wireless Communications and Networking, vol. 2004, no. 2, pp. 222-235, December 2004.
- [42] W. Mennerich and W. Zirwas, *Implementation issues of the partial CoMP concept*, IEEE PIMRC, pp. 1939-1944, September 2010.
- [43] C.-H. Yu, S. Qin, M. Alava, and O. Tirkkonen, *Distributed graph clustering for application in wireless networks*, Springer Berlin Heidelberg IWSOS, pp. 92-103, 2011
- [44] S. Qin, C.-H. Yu, O. Tirkkonen, and M. Alava, *Distributed Coordination Area Formation in Coordinated Multi-Point Transmission*, IEEE GLOBECOM, pp. 1-5, December 2011.
- [45] J. Zhang, R. Chen, J. Andrews, A. Ghosh, and R. Heath, *Networked MIMO with clustered Linear Precoding*, IEEE Trans. on Wireless Commun., vol. 8, no. 4, pp. 1910-1921, April 2009.
- [46] M. Joham, W. Utschick, and J. Nossek, *Linear Transmit Processing in MIMO Communication Systems*, IEEE Trans. on Signal Processing, vol. 53, no. 8, pp. 2700-2712, August 2005.
- [47] T. Yoo and A. Goldsmith, *On the optimality of multiantenna broadcast scheduling using zero-forcing beamforming*, IEEE J. Select. Areas Commun., vol. 24, no. 3, pp. 528-541, March 2006.
- [48] M. Grote and T. Huckle, *Parallel Preconditioning with Sparse Approximate Inverse*, SIAM Journal on Scientific Computing, vol. 18, no. 3, pp. 838-853, May 1997.
- [49] 3GPP TR 36.814 v.9.0.0, *Further advancements for E-UTRA physical layer aspects*. [Online] Available: www.3gpp.org.

Appendices

A Least Squares Problem

A least squares problem is a norm square minimization problem without a constraint:

$$\text{minimize } \|\mathbf{A}\mathbf{x} - \mathbf{b}\|_2^2 \quad (39)$$

where $\mathbf{A} \in \mathcal{R}^{m \times n}$, and $\mathbf{x}, \mathbf{b} \in \mathcal{R}^m$.

The solution to least squares problem can be solved in different ways. A closed form solution is given as:

$$\begin{aligned} (\mathbf{A}^T \mathbf{A})\mathbf{x} &= \mathbf{A}^T \mathbf{b} \\ \mathbf{x} &= (\mathbf{A}^T \mathbf{A})^{-1} \mathbf{A}^T \mathbf{b} \end{aligned} \quad (40)$$

Another solution to least squares could be found using a QR-decomposition method. Let us have the QR-decomposition of \mathbf{A} as:

$$\mathbf{A} = \mathbf{Q} \begin{bmatrix} \mathbf{R} \\ \mathbf{0} \end{bmatrix} \quad (41)$$

where $\tilde{\mathbf{Q}} \in \mathbb{R}^{m \times m}$ is an orthonormal matrix, $\tilde{\mathbf{R}} \in \mathbb{R}^{n \times n}$ is an upper triangular matrix and $\mathbf{0}_{(m-n) \times n}$ is a zero matrix. The solution is then given as

$$\mathbf{x} = [\mathbf{R}^{-1} \quad \mathbf{0}_{n \times (m-n)}] \mathbf{Q}^H \mathbf{b} \quad (42)$$

A third approach to solve the least squares problem is using SVD. However, since we are interested in this approach, it is not covered in this appendix.